



Multistability and Transient Dynamics on Networked Systems

Der Fakultät für Mathematik & Naturwissenschaften
der Carl von Ossietzky Universität Oldenburg
zur Erlangung des Grades und Titels
Doktor der Naturwissenschaften (Dr. rer. nat.)
angenommene Dissertation

von

Kalel Luiz Rossi

geboren am 13.10.1997 in Curitiba, Parana, Brasilien

Gutachter:

Gutachter:

Tag der Disputation:

Contents

List of Publications	4
1 Small changes at single nodes can shift global network dynamics	6
1.1 Introduction	6
1.2 Methodology	8
1.3 Results	10
1.3.1 Introduction to dynamical malleability	10
1.3.2 Comprehensive view of dynamical malleability	12
1.3.3 Unpredictability of dynamical malleability	15
1.3.4 Ratio of short to long-range connections	16
1.3.5 Multistability	17
1.3.6 Distributions of samples	22
1.4 Discussions and conclusions	22
2 Conclusions	28
Acknowledgments	42
Eidesstattliche Erklärung	43

List of Publications

This dissertation is based on the following publications:

Chapter 2.1.7: George Datseris, Kalel L. Rossi, and Alexandre Wagemakers. Framework for global stability analysis of dynamical systems. *Chaos* **33**, 073151 (2023).

Statement of authorship:

George Datseris: Conceptualization (lead); Investigation (equal); Formal analysis (equal); Software (equal); Visualization (lead); Writing – original draft (equal); Writing – review & editing (equal).

Kalel Luiz Rossi: Conceptualization (equal); Formal analysis (equal); Software (equal); Visualization (equal); Writing – original draft (equal); Writing – review & editing (equal).

Alexandre Wagemakers: Conceptualization (equal); Formal analysis (equal); Software (equal); Writing – original draft (equal); Writing – review & editing (equal).

Chapter 3: Kalel L. Rossi, Roberto C. Budzinski, Bruno R. R. Boaretto, Lyle E. Muller, and Ulrike Feudel. Small changes at single nodes can shift global network dynamics. *Physical Review Research* **5**, 013220 (2023).

Statement of authorship:

Kalel Luiz Rossi: Conceptualization (equal); Investigation (lead); Formal analysis (lead); Software (lead); Visualization (lead); Writing – original draft (lead); Writing – review & editing (lead).

Roberto C. Budzinski: Conceptualization (equal); Investigation (equal); Formal analysis (equal); Writing – original draft (equal); Writing – review & editing (equal).

Bruno R. R. Boaretto: Conceptualization (equal); Investigation (equal); Formal analysis (equal); Writing – original draft (equal); Writing – review & editing (equal).

Lyle E. Muller: Conceptualization (equal); Investigation (equal); Formal analysis (equal); Writing – review & editing (equal).

Ulrike Feudel: Conceptualization (equal); Investigation (equal); Formal analysis (equal); Writing – original draft (equal); Writing – review & editing (equal); Supervision (lead).

Chapter 4: Kalel L. Rossi, Everton S. Medeiros, Peter Ashwin and Ulrike Feudel. Transients versus network interactions give rise to multistability through trapping mechanism. In preparation.

Statement of authorship:

Kalel Luiz Rossi: Conceptualization (equal); Investigation (lead); Formal analysis (lead); Software (lead); Visualization (lead); Writing – original draft (lead); Writing – review & editing (lead).

Everton S. Medeiros: Conceptualization (equal); Investigation (equal); Formal analysis (equal); Writing – original draft (equal); Writing – review & editing (equal).

Peter Ashwin: Investigation (supporting); Formal analysis (equal); Writing – review & editing (equal).

Ulrike Feudel: Conceptualization (equal); Investigation (equal); Formal analysis (equal); Writing – original draft (equal); Writing – review & editing (equal); Supervision (lead).

Chapter 5: Kalel L. Rossi, Roberto C. Budzinski, Everton S. Medeiros, Bruno R. R. Boaretto, Lyle E. Muller, and Ulrike Feudel. Dynamical properties and mechanisms of metastability: a perspective in neuroscience. Submitted.

Statement of authorship:

Kalel Luiz Rossi: Conceptualization (equal); Investigation (lead); Formal analysis (lead); Software (lead); Visualization (lead); Writing – original draft (lead); Writing – review & editing (lead).

Roberto C. Budzinski: Conceptualization (equal); Investigation (equal); Formal analysis (equal); Writing – original draft (equal); Writing – review & editing (equal).

Everton S. Medeiros: Conceptualization (equal); Investigation (equal); Formal analysis (equal); Writing – original draft (equal); Writing – review & editing (equal).

Bruno R. R. Boaretto: Conceptualization (equal); Investigation (equal); Formal analysis (equal); Writing – original draft (equal); Writing – review & editing (equal).

Lyle E. Muller: Conceptualization (equal); Investigation (supporting); Formal analysis (supporting); Writing – review & editing (equal).

Ulrike Feudel: Conceptualization (equal); Investigation (equal); Formal analysis (equal); Writing – original draft (equal); Writing – review & editing (equal); Supervision (lead).

On top of these main thesis papers, I have also collaborated in other works, which resulted in two further publications, with me as a co-author. They are not included in this thesis.

- Bruno R. R. Boaretto, Roberto C. Budzinski, Kalel L. Rossi, Thiago L. Prado, Sergio R. Lopes and Cristina Masoller. Temporal Correlations in Time Series Using Permutation Entropy, Ordinal Probabilities and Machine Learning. *Entropy* **23**, 1025 (2021).
- Bruno R.R. Boaretto, Roberto C. Budzinski, Kalel L. Rossi, Cristina Masoller, Elbert E.N. Macau. Spatial permutation entropy distinguishes resting brain states. *Chaos, Solitons and Fractals* **171**, 113453 (2023).

Chapter 1

Small changes at single nodes can shift global network dynamics

Abstract

Understanding the sensitivity of a system's behavior with respect to parameter changes is essential for many applications. This sensitivity may be desired - for instance, in the brain, where a large repertoire of different dynamics, particularly different synchronization patterns, is crucial - or may be undesired - for instance, in power grids, where disruptions to synchronization may lead to blackouts. In this chapter¹, we show that networks of coupled phase oscillators with nonlinear interactions can acquire a very large and complicated sensitivity to changes made in either their units' parameters or in their connections. Even modifications made to a parameter of a single unit can radically alter the global dynamics of the network in an unpredictable manner. This occurs over a wide parameter region, around the network's transitions to phase synchronization. We argue that this is a widespread phenomenon that can be expected in real-world systems, extending even beyond networks of oscillators.

1.1 Introduction

Several systems of practical and theoretical importance are composed of, or can be modeled as, networks of interacting units. Examples from different research areas include power grids (networks of producers and consumers of electrical energy) [1], food webs [2], networks of electronic elements [3], coupled lasers [4], and neurons in the brain [5]. An important question is how the dynamics of single units impact the network's overall dynamics, and what happens if these units are modified. What happens to the dynamics if the units' parameters change? For instance, in ecological systems, what happens if the reproduction rate of a prey increases? In power grids, can a change in the parameters of a single generator cause a large disruption, such as a blackout? Also, what happens if the units' dynamical states are modified, e.g. by shocking the units into a different state? In the brain, how can an epileptic seizure be stopped by employing a current pulse in one particular brain region? These questions highlight the idea that a regime in which single-unit-changes can alter the whole network's behavior can be either dangerous or advantageous, and is an important topic of research which we address in this work.

In both power grids and the brain, an important phenomenon is synchronization, i.e. the coherence of frequencies or even phases of oscillations. For example, it is crucial for power grids to have their elements synchronized in the 50 – 60 Hz regime [6]. Moreover, several functional roles have been ascribed to synchronization in the brain [7, 5, 8]. For systems in which synchronization is an essential process for functioning, the question of

¹This chapter is a modified form of a published manuscript: Kalel L. Rossi, Roberto C. Budzinski, Bruno R. R. Boaretto, Lyle E. Muller, and Ulrike Feudel. *Physical Review Research* **5**, 013220 (2023).

sensitivity with respect to perturbations becomes particularly important. This has been recognized in the literature, and various types of perturbations have been considered to study the vulnerability either of the synchronized state itself or of the transition to synchronization [9, 10].

In this work, we show that systems become very sensitive to changes in parameters during transitions to synchronization, such that even changes to parameters of single units can radically alter the dynamics of the whole system. We call this phenomenon *dynamical malleability* [11], characterized by the fluctuations in network behavior caused by changes in the units' parameters or connections. Dynamical malleability can cause problems in real-world systems in two major ways: (i) the fluctuations in the dynamics can have a large magnitude, which can lead to drastic changes in the system's spatiotemporal dynamics and (ii) fluctuations are complicated and hard to predict, so that it is unclear which units or new parameter values can keep the networks in a similar synchronization state, and which others can not. Indeed, no method available in the literature to describe phase synchronization worked satisfactorily to predict the fluctuations we observe. This clearly important issue for the design and control of systems motivates our study to analyze the mechanisms that lead to these large fluctuations.

To address it concretely, we study networks of Kuramoto oscillators organized in ring lattices. They constitute a paradigmatic model for synchronization [12, 13, 14] and have been established as a model for real-world systems like the brain [15, 16, 14], Josephson junctions [17, 3], and chemical oscillators [18, 19]. The Kuramoto oscillators are phase oscillators coupled through a sine function of their phase differences. Networks with these units are well-known to have a transition from desynchronization (incoherent phases) to frequency synchronization (i.e. phase-locking, meaning constant phase differences [9]) and to phase synchronization (small phase differences) [20] as the coupling strength between units increases [14, 13].

In this work, we connect the oscillators in either of two classes of network topologies, which are of theoretical and practical importance [21]: Watts-Strogatz [22, 23, 24] and distance-dependent [25, 26]. They have very distinct properties, but in both a change in the topology from short-range to long-range connections leads to a transition to phase synchronization in the networks [27, 25]. During the transitions to phase synchronization, when the systems are only partially phase synchronized, they become dynamically malleable (i.e., sensitive to parameter changes), as illustrated in Fig. 1.1.

Furthermore, we also show that the number of attractors of the Watts-Strogatz networks increases during their transitions to phase synchronization, meaning that these systems also become especially sensitive to perturbations made to their units' states. This goes in line with recent studies for Kuramoto oscillators with identical frequencies [28, 29, 30] and for Kuramoto oscillators with inertia [31]. This increased multistability acts as a dynamical mechanism that can further increase the dynamical malleability.

Therefore, despite the wide literature and importance of synchronization, this phenomenon we describe of increased sensitivity to parameter changes, with complicated, hard-to-predict consequences to the synchronization, and which can be accompanied by multistability, has so been under-explored in the literature. Although reported sporadically in some recent works [32, 33, 34, 35], it has not been the focus, and thus has not been fully explored, until now. This becomes especially relevant when we note that the behavior is widespread, extending well beyond the Kuramoto networks studied here, as supported by our observations in a variety of topologies, by similar observations in spiking [11] and bursting [35] neural networks, in cellular automata (which we exemplify

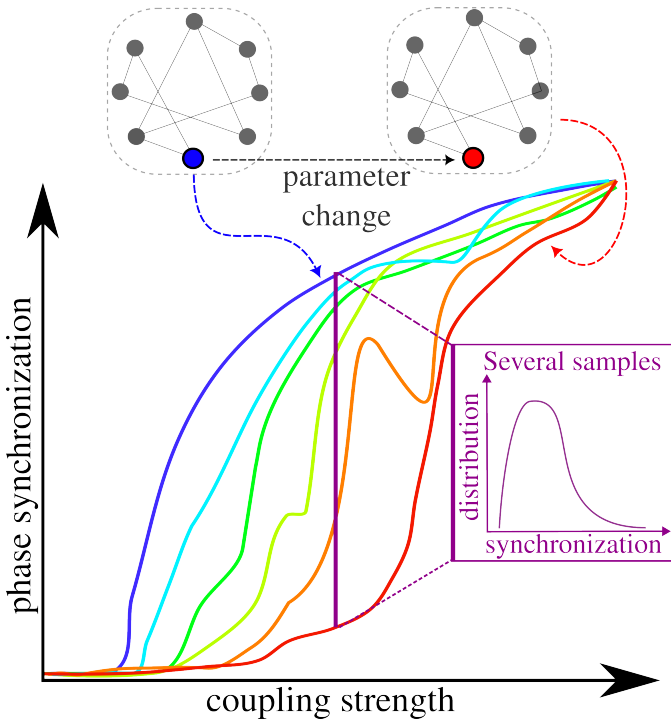


Figure 1.1: **Sketch to illustrate the dynamical malleability in a typical transition to phase synchronization.** Each realization of the system’s parameters leads to a different transition to synchronization, i.e. a different curve in the figure. Realizations may differ from the others, for instance, in the parameter of a single unit. We see that the transitions to synchronization are different, as both the critical value of the coupling strength and the profile of the transitions differ, with the magnitude of malleability peaking during the transitions. Fixing the coupling strength, we can also look at the distribution of the degree of phase synchronization across samples (purple inset).

in the Supplemental Material), and, importantly, by the statistical physics theory of finite-size effects on phase transitions, which we discuss later in the chapter.

We therefore hope to demonstrate the importance of dynamical malleability, and to encourage further theoretical advancements in this area, which are needed to properly describe the wide range of behaviors and to offer tools for practical applications.

1.2 Methodology

In the Kuramoto model [12, 36], each oscillator is described by a phase which evolves in time according to

$$\dot{\theta}_i = \omega_i + \epsilon \sum_{j=1}^N A_{ij} \sin(\theta_j - \theta_i), \quad (1.1)$$

where $\theta_i(t)$ is the phase of the i -th oscillator at time t , ω_i is its natural frequency, ϵ is the coupling strength, N is the number of oscillators, and A_{ij} is the (i, j) -th element of the adjacency matrix \mathbf{A} . Throughout this work, we initially draw each frequency randomly from a Gaussian distribution with mean $\mu = 0.0$ and standard deviation $\sigma = 1.0$, generating a sequence $\{\omega_i\}, i = 1, \dots, N$. Then, different realizations can (i)

shuffle these frequencies, generating another sequence $\{\omega_i\}_{\text{shuffled}} = \text{shuffle}(\{\omega_i\})$; or (ii) switch the frequency of one selected unit to another value ω_{new} .

The networks in this work are coupled in a ring lattice of $N = 501$ units with periodic boundary conditions, and follow one of two classes of topology. The first class is the Watts-Strogatz (WS) [22], which interpolates between regular and random topologies with a parameter p , the rewiring probability: at one extreme ($p = 0$), the topology is a k -nearest-neighbor lattice. From it, connections are randomly chosen according to the probability p and rewired to another randomly chosen connection. In doing this, the networks have a significant decrease in the mean distance between nodes, but remain very clustered, generating small-world topologies. The other extreme ($p = 1$) is then a random topology. These networks are unweighted, so their adjacency matrix's elements are $A_{ij} = 1$ if i and j are connected, and 0 otherwise.

The second class of networks follows a distance-dependent (DD) powerlaw scheme, in which any given node receives connections with weights decaying based on the distance to it. Each element of the adjacency matrix is $A_{ij} = \frac{1}{\eta(\alpha)(d_{ij})^\alpha}$, where d_{ij} is the edge distance between oscillators i and j , defined as $d_{ij} = \min(|i - j|, N - |i - j|)$, and $\eta(\alpha)$ is a normalization term given by: $\eta(\alpha) = \sum_{j=1}^{N'} \frac{2}{j^\alpha}$, such that the temporal evolution of the phases can be written as:

$$\dot{\theta}_i = \omega_i + \frac{\epsilon}{\eta(\alpha)} \sum_{j=1}^{N'} \frac{1}{j^\alpha} [\sin(\theta_{i+j} - \theta_i) + \sin(\theta_{i-j} - \theta_i)], \quad (1.2)$$

where $N' = \frac{N-1}{2}$ denotes half the amount of units to which i is connected to (one half of the ring's length, discounting the unit i itself). The equation explores the symmetry in the network to switch the summation across the network to a summation across only half, multiplied by 2. The powerlaw decay is thus controlled by α , the locality parameter. For $\alpha = 0$, the network is globally coupled with equal weights between every node. As α increases, the weights are redistributed, so that closer units (in terms of edge-distance) have bigger weights. At the extreme of $\alpha \rightarrow \infty$, only first-neighbors are connected.

The two classes have similarities: they have topologies dominated by short-range connections at one extreme and by long-range connections at another [37, 38]. They also have differences: the first class is sparsely connected, the other densely; the first has link-disorder (different rewirings lead to different networks), the second does not.

Integration was performed using the Tsitouras 5/4 Runge-Kutta (Tsit5) method for Watts-Strogatz networks, and an adaptive order adaptive time Adams Moulton (VCABM) method for distance-dependent networks. The integrator method was chosen for distance-dependent networks for increased simulation speed, and results were robust to different integration schemes. All methods used the DifferentialEquations.jl package [39], written in the Julia language [40]. Additional computational packages used were PyPlot [41] for plotting and DrWatson.jl [42] for code management. The code used for simulations is accessible in the repository [43], with the parameters used in the simulations. In particular, the control parameters we used (α , p and ϵ) were generated from a uniform distribution in the range of parameters showing interesting behaviors (e.g. the transitions to synchronization), then rounded to five decimal places and used in the simulations (in the case of p , the distribution was uniform in the log scale). These values are reported in all figures and text, and we emphasize that no value was chosen specifically by hand: the behaviors we show in the figures are typical of the systems and

can be obtained by randomly generating other values for the parameters.

We quantify the degree of phase synchronization of the network through the standard Kuramoto order parameter [12, 36, 13], which is the circular average of the units' phases

$$r(t) = \frac{1}{N} \left| \sum_{j=1}^N \exp(i\theta_j(t)) \right|, \quad (1.3)$$

with $i = \sqrt{-1}$. The quantifier ranges from 0 to 1: if $r(t) = 1$, all the phases are the same, and the system is completely globally phase-synchronized; if $r(t) = 0$, each oscillator has a pair that is completely out-of-phase, and the system can be completely globally phase-desynchronized or in a twisted state with units having distinct but linearly spaced phases. We typically describe networks by the temporal average $R := \frac{1}{T} \sum_t r(t)$ of their phase synchronization, with T being the total simulation time excluding transients.

1.3 Results

1.3.1 Introduction to dynamical malleability

The networks we study here, described in Eq. (1.1), follow the basic phenomenology of transitions to synchronization in Kuramoto networks [12, 13]. For very small coupling strengths ϵ , the oscillators are effectively uncoupled, and the phases oscillate without any significant correlation. As this ϵ increases, the instantaneous frequencies $\dot{\theta}_i$ align first, and the units' phases become locked, but not aligned: the system becomes frequency but not phase synchronized [9].

Then, whether the phases can align or not depends on the topology [44, 27]. In a two-nearest neighbor lattice, where only four nearby units are connected (two on each side), there is a topological limitation in the spread of interactions across the network that makes the oscillators arrange themselves in shorter-range patterns (Fig. 1.2(a)) (an exception might occur if the coupling strength is extremely high, much bigger than the relevant values studied here). If the short-range connections are randomly rewired to long-range connections, following for instance the Watts-Strogatz (WS) algorithm, the shorter-range patterns give way to longer-range patterns, and the oscillators start to phase synchronize ((b) and (c)), until eventually a strong (though not complete) phase synchronization (PS) is reached (d). This occurs at different stages for each realization: for instance, panels (c) and (k) reach a high degree of PS, with the longer-range patterns, but panel (g) does not.

In Fig. 1.2, the natural frequencies $\{\omega_i\}(i = 1, \dots, N)$ were kept constant across panels (a)-(d). Changing the frequencies, keeping the initial conditions $\{\theta_i(0)\}(i = 1, \dots, N)$ fixed, leads to a different realization (also called sample), with possibly different dynamics. If the frequency of a single unit ω_i is changed to an arbitrary new value, for instance $\omega_{\text{new}} = 3$, the network's behavior can be significantly altered (panels (e)-(h)). This is especially the case for networks with intermediate rewiring probabilities p , in which this single unit frequency change can bring the network from high to very low phase synchronization (panels (c) to (g)). The instantaneous frequencies typically remain synchronized, though their values might change. For random networks, phase synchronization is always maintained, though the instantaneous frequency values may also change.

Figure 1.2 thus illustrates that the long-term dynamics and phase synchronization differ in each realization. The realizations, created by changing the natural frequency of

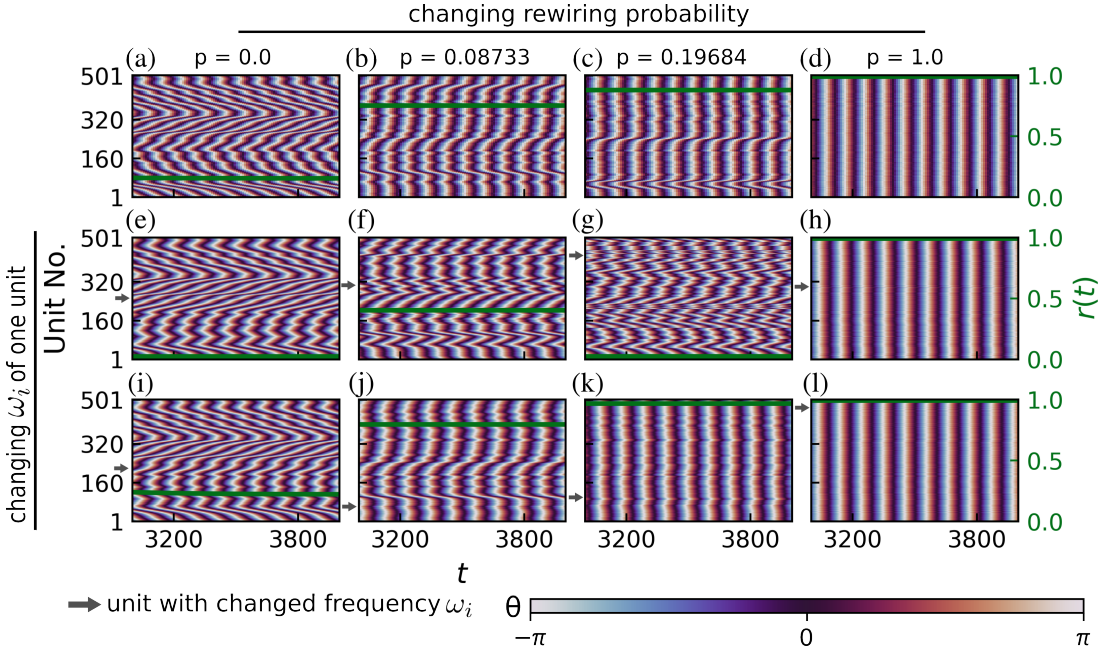


Figure 1.2: Transition to phase synchronization and the effect of a single-unit change. The figure shows the color-coded phases θ of all oscillators in the network and the degree of phase synchronization $r(t)$ (green line) across time for Watts-Strogatz networks. The coupling strength ϵ is fixed at $\epsilon = 4.51282$ and the natural frequencies ω_i in the first row are the same, generated by randomly drawing from a Gaussian distribution with zero mean and unitary standard deviation. Networks in the left column are two-nearest-neighbor lattices (rewiring probability $p = 0$); the short-range connections in these networks are then rewired in the following columns, with probability $p = 0.08733$ in the second column, $p = 0.19684$ in the third, and $p = 1.0$ in the fourth (leading to random networks). Increasing the proportion of long-range connections thus leads generally to more phase-synchronized networks. In the second and third rows, the natural frequency ω_i of a single unit i (indicated by the gray arrows) is changed to a new value $\omega_i \rightarrow \omega_{\text{new}} = 3.0$, with all other parameters being kept fixed. The units shown in the figure were those which led to the smallest (second row) or highest (third row) degree of phase synchronization R out of all $N = 501$ units in the network for each value of p . Initial conditions were the same for all simulations, and were randomly drawn between 0 and 2π .

one unit, are distinct dynamical systems, so it is not surprising to observe distinct long-term dynamics. It is, however, interesting to observe how large these changes in dynamics can be, and how they depend on the topology. For instance, in networks of intermediate p (second and third columns of Fig. 1.2), the phase synchronization changes drastically. In random networks ($p = 1$, fourth column), they preserve the phase synchronization but alter the instantaneous frequencies of the oscillators (seen in the figure by the number of vertical lines). We also note that the behavior we describe is typical of the systems, and the values of p and ϵ used here were generated as described in Section 1.2. Since the fluctuations in the phase patterns (reflected in the phase synchronization) are clearer and more pronounced than the instantaneous frequency patterns, we now focus on the phase synchronization of the networks.

1.3.2 Comprehensive view of dynamical malleability

To obtain a comprehensive picture we now study an ensemble of samples obtained by shuffling the frequencies ($\{\omega_i\}_{\text{original}} \rightarrow \{\omega_i\}_{\text{shuffled}} = \text{shuffle}(\{\omega_i\}_{\text{original}})$) or by changing the frequency of only a single unit to a new value ($\omega_{i,\text{original}} \rightarrow \omega_{\text{new}}$). We show in Fig. 1.3 the transitions to phase synchronization with increasing coupling strength or with switching from short-range to long-range connections. As expected from Fig. 1.2 we also find a large dynamical malleability (sometimes simply called malleability) during the transitions.

We study two classes of topology, Watts-Strogatz (WS, small-world) and distance-dependent (DD), described in Sec. 1.2. We consider ensembles as collections of networks with fixed coupling strength ϵ and topology (fixed rewiring probability p or locality parameter α) but distinct realizations of the natural frequencies $\{\omega_i\}$ [45]. Each ensemble in the figure contains 501 samples (realizations). We present the results using the mean degree of phase synchronization R for each realization, and the gap $\Delta := R_{\max} - R_{\min}$ between the most and least phase synchronized realizations in each ensemble. The gap Δ is chosen simply to illustrate the wide range of R values clearly, and we remark that very similar curves are observed by using the standard deviation over samples.

In Fig. 1.3, thicker lines represent an “original” sequence of frequencies $\{\omega\}_{\text{original}}$, from which other realizations (light lines) are created by shuffling all frequencies or changing the frequency of one unit to a new value $\omega_{\text{new}} = 3.0$. Each sample is a different dynamical system, and has a different transition to phase synchronization, which occurs at different values of ϵ , p , or α , and with a different profile (some have a small region of desynchronization while others do not, for instance).

This means that changing samples can lead to large changes in the behavior of the system, as we see throughout Fig. 1.3. First, we study the transitions induced by increasing the coupling strength ϵ for four representative types of networks (panels (a)-(d)), characterized by four specific values of rewiring probability p and locality parameter α .

In the red curves, networks are dominated by long-range connections, with $p = 1$ (random) and $\alpha = 0$ (all-to-all) and have a complete transition to phase synchronization (reaching $R \sim 1$), with the dynamical malleability (measured by Δ) increasing during the transition and returning to zero after. The all-to-all case is the finite-size version of the system originally studied by Kuramoto [36], and the critical ϵ values, when the transition occurs in each sample, are close to the $\epsilon_c = \frac{2}{g(0)\pi} = \frac{2\sqrt{2}}{\sqrt{\pi}} \approx 1.596$ predicted in the thermodynamic (infinite network size) limit. Its finite-size scaling properties and behavior have also been studied in [46, 32]. It is worth mentioning that this parallel between random networks and all-to-all networks, which have similar phenomenology, has been described in other works. Both have the same scaling exponents, belonging to the mean-field type [37, 38].

In the green curves ($p = 0.19684$ and $\alpha = 1.538463$) some connections have been rewired in the Watts-Strogatz networks, and weights redistributed for distance-dependent networks, from long-range to effectively short-range connections. On average, phase synchronization R decreases, though still remaining high. Some samples of WS networks also start to display regions of desynchronization: after the initial transition to high R , a further increase in ϵ can desynchronize them (visible in panels (a) and (c), for ϵ roughly in [6, 7]). Therefore, the huge changes in R ($\Delta \sim 0.99$) due to changing samples can be attributed to two effects: the difference in their critical coupling strength (when the

transition begins) [47], and also in their different post-transition behaviors (such as the desynchronization gaps that occur at different intervals of ϵ .)

In the purple curves ($p = 0.08733$ and $\alpha = 1.76923$), even more short-range connections become present. Phase synchronization R on average decreases, while the fluctuations Δ remain high and occur more evenly spread across samples.

Finally, for cyan curves ($p = 0$, two-nearest-neighbor chains and $\alpha = 3$, close to nearest-neighbor chains), the connections are short-range. Their phase synchronization is much smaller, and they do not reach a high degree of phase synchronization for any value ϵ we tested. These networks with short-range connections still have some degree of malleability, but not as high as the previous two cases.

Returning to frequency synchronization, we mention that for weak coupling strengths (roughly below $\epsilon \approx 3$), most of the samples in any ensemble are not frequency synchronized (see Fig. S3). Above this value, frequency synchronization becomes more common, especially for networks with more long-range connections, such that for sufficiently high coupling all samples become frequency synchronized. This is not the case for networks with mostly short-range connections ($p \lesssim 0.01$), in which some samples do not reach frequency synchronization even despite strong coupling. The presence of frequency synchronization in the short-range networks is consistent with the literature [48, 13] showing that frequency synchronization in first-nearest-neighbor chains is possible for sufficiently high ϵ in strictly finite systems. There are therefore also sample-to-sample fluctuations in the frequency synchronization of Kuramoto networks. They occur similarly to the fluctuations in phase synchronization, but are somewhat harder to visualize and have a less interesting dependence on parameters, justifying our focus on phase synchronization in this chapter.

We now move to the topology induced transitions, which occur by switching from short-range to long-range connections (varying p and α) while keeping the coupling strength ϵ fixed (Figs. (e-h)). A similar scenario occurs with a transition to phase synchronization, induced by changing either p or α . The dynamical malleability increases during the transitions, reaching significant values for both shuffled realizations and single-unit changes. The nearest-neighbor networks show some malleability, while the long-range dominated ones (random or all-to-all) show no malleability. We note here that the transition for WS occurs at $p \sim 0.1$, so we plot the figures on logarithmic scale to show the full transition to synchronization. This transition was already reported for WS networks in [27], but the authors used a linear scale for p and missed the full details of the transition that we see here, especially the sample-to-sample fluctuations; for distance-dependent powerlaw networks, a transition in phase and frequency was reported in [25]. However, none of these references studied the sample-to-sample fluctuations.

We conclude that either shuffling or changing a single unit can significantly alter the behavior of these systems, leading to a large dynamical malleability, in some cases over a very large range of parameters. This is particularly strong for WS networks, reaching $\Delta \sim 0.99$, close to the maximum possible value of $\Delta = 1.0$. The distance-dependent networks have weaker fluctuations, though still significant, reaching up to $\Delta \sim 0.7$.

Furthermore, we note that the networks with intermediate p or α and the short-range networks have dynamical malleability even for high ϵ . This is consistent with the known increase in the fluctuations near a phase transition [46, 49, 50] because the networks with these parameters remain close to the topology-induced transition. This is illustrated for WS networks in Fig. 1.4. It shows, in the $p-\epsilon$ parameter space, the average phase synchronization across samples \bar{R} on the first panel and the dynamical

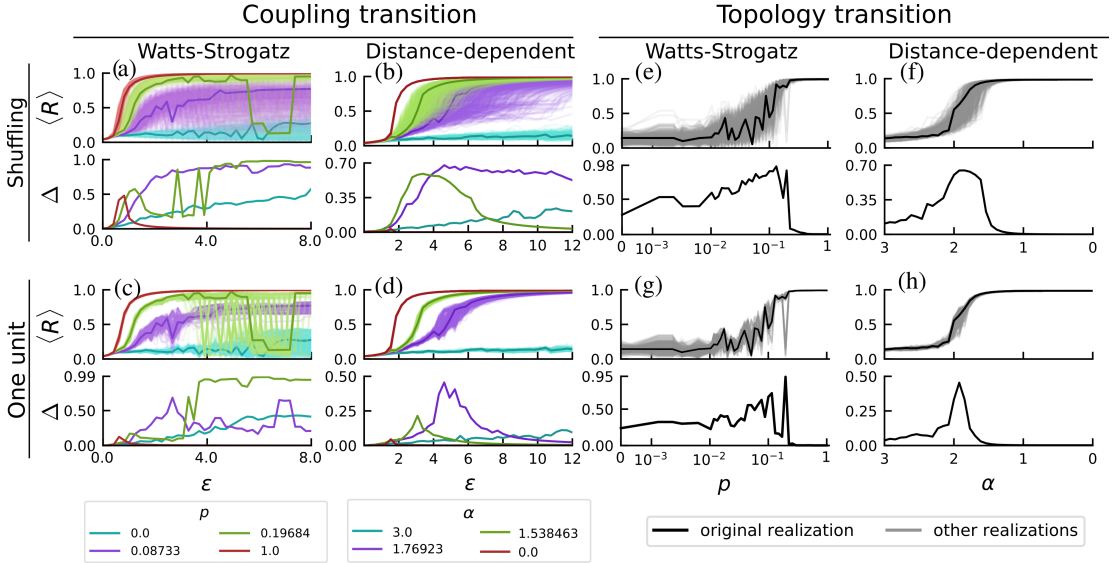


Figure 1.3: Transitions to phase synchronization and dynamical malleability. Networks under Watts-Strogatz (WS) and distance-dependent (DD) topologies reach phase synchronization through either an increase in coupling strength ϵ (given the topology has a sufficient amount of long-range connections) or by switching short-range connections to long-range. Fluctuations in the degree of phase synchronization R between samples increase during the transitions, as can be seen by the differences in the same-colored curves and by $\Delta := R_{\max} - R_{\min}$. Starting from a natural frequency sequence originally drawn from a Gaussian distribution (thicker lines), the other samples (thinner lines) can be generated by shuffling the natural frequencies or by switching the natural frequency of one unit to $\omega_{\text{new}} = 3$. For intermediate networks (purple and green curves), the increase in the fluctuations (i.e. in dynamical malleability) extends for a wide range of parameters and becomes considerably large. Each panel contains $501 = N$ realizations, with rewiring probabilities fixed for the coupling transition, with values shown in the legend, and coupling strength fixed in the topology transition at $\epsilon = 4.51282$ for WS and $\epsilon = 6.46154$ for DD. The initial conditions are the same across all realizations, and are randomly distributed from 0 to 2π . The curves of Δ are qualitatively similar with other dispersion measures, such as standard deviation, a possible difference being that the curves may be slightly shifted, as the measures can peak at slightly different values of the control parameter. We remark that the parameter values used in the simulations were generated as described in Section 1.2 and correspond to the typical behaviors in the system.

malleability measured by Δ on the second panel. Figure 1.4 provides a comprehensive view on both the coupling strength and the topology-induced transitions. The samples are realized here as shuffles, though a similar figure would be obtained by changing one unit. There is a single region of phase synchronization for sufficiently high coupling strength ϵ and rewiring probability p (panel (a)). Around the borders of this region, where the system is transitioning, the dynamical malleability is much higher (panel (b)). It then becomes clear that the intermediate networks (green and purple lines), are near the topology-induced transition (for instance, black line) for all $\epsilon \gtrsim 1$. As ϵ increases, the networks remain near this p -transition, and so their dynamical malleability

does not decrease. For the regular networks, we first note that the p -axis is shown on a logarithmic scale, such that these networks, with $p = 0$, are still relatively close to the transition at $p_c \approx 0.1$, and thus they also present significant malleability.

Figure 1.4 also illustrates the existence of two qualitatively different types of transitions: one induced by increasing coupling strength (for sufficiently high p), and another induced by increasing p (for sufficiently high ϵ). The difference between both is in their starting points. Both are globally phase desynchronized, but in the former (red, green, and purple lines), the weak coupling strength regimes have mostly uncorrelated oscillators, with no discernible structures in the phases or even synchronization in the frequencies. In the latter (black line), there are shorter-range structures with frequency synchronization for most samples.

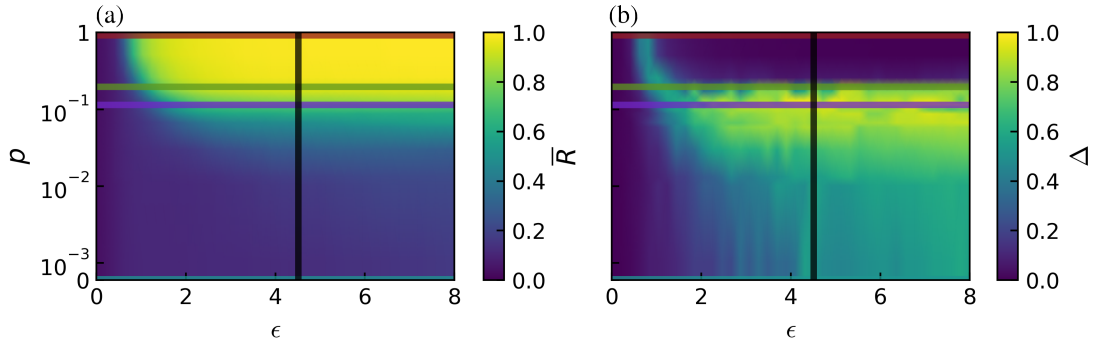


Figure 1.4: Dynamical malleability increases around the regions of transition to phase synchronization. The surface on the left shows the average degree of phase synchronization \bar{R} across the ensemble (1000 realizations of shuffled natural frequencies). The region of high phase synchronization is clearly seen for sufficiently high coupling strength ϵ and rewiring probability p . The colored lines correspond to the parameter values shown in Fig. 1.3. The right panel displays Δ , the difference between the most and least synchronized realizations for each pair (p, ϵ) , and we see that the fluctuations from sample to sample increase during the transitions to phase synchronization. The green and purple curves remain close to the region of transition for all $\epsilon \gtrsim 1$, such that their fluctuations do not decrease with an increase in ϵ . The figure uses Gouraud interpolation to ease visualization by smoothing the curves with a linear interpolation.

1.3.3 Unpredictability of dynamical malleability

For Watts-Strogatz networks, samples can be generated by resampling the topology instead of changing the natural frequencies. Since they are generated by a random rewiring process, different realizations generate different networks (there is link-disorder [38]). Therefore, different samples can also be generated by resampling the network while keeping the natural frequencies fixed. This generates a profile of dynamical malleability similar to that shown in Fig. 1.3(e), where the network was fixed and the natural frequencies were changed (see Fig. S1 for details).

Now, we wish to illustrate that no network, or natural frequency sequence, is alone responsible for leading to more, or less, synchronized states. Instead, the samples depend sensitively on both, especially in the region of large STS fluctuations. Figure 1.5(a) shows the degree of phase synchronization for different realizations of the networks and different shuffles of the natural frequencies, all for $\epsilon = 4.51282$ and $p = 0.08733$ with

fixed initial conditions. To aid the visualization, red rectangles indicate the network with the largest R for each shuffle. No network synchronizes more (or less) for any sequence of natural frequencies; and no sequence of natural frequencies synchronizes more for any network. Furthermore, if the ϵ , p , or initial condition are changed, the whole profile of the figure also changes. Another way to illustrate the complicated sensitivity in the

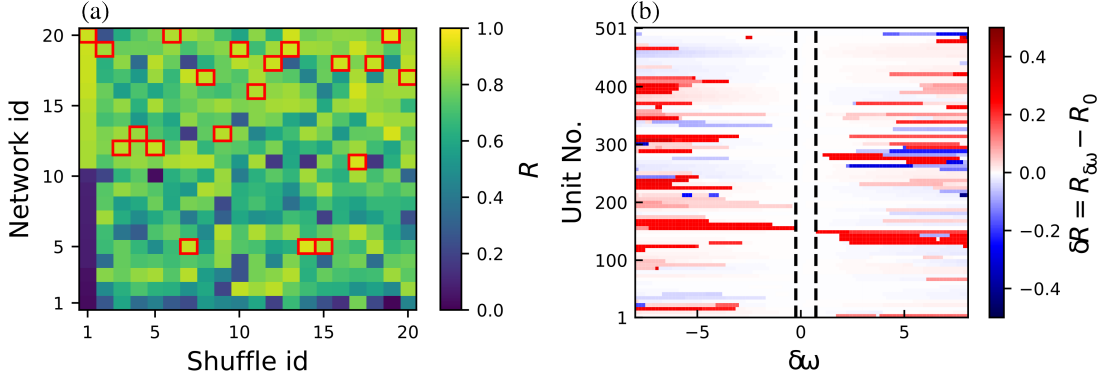


Figure 1.5: Fluctuations in dynamically malleable systems are unpredictable. Panel (a) shows the average phase synchronization R for fixed coupling strength $\epsilon = 4.51282$ and rewiring probability $p = 0.08733$ for different 20 shuffles of the natural frequencies $\{\omega_i\}$ and samples of networks generated by the Watts-Strogatz algorithm. For ease of visualization, the networks are ordered such that the highest network ids correspond to higher synchronization for Shuffle id = 1. For each shuffle, the network with the highest R is marked with a red rectangle. We thus see that no network synchronizes more for all shuffles: R is a function of both the specific frequency and topology samples. Panel (b) shows the changes δR in the phase synchronization R when the natural frequency of each unit is changed by an amount $\delta\omega$, such that $\omega_i \rightarrow \omega_i + \delta\omega$. Other parameters are fixed, in particular $p = 0.1145$ and $\epsilon = 4.51282$. There is a rough threshold (indicated by the black dashed lines), below which changing ω_i does not significantly alter R ($\delta R < 0.1$ for the figure). Furthermore, changing the frequency does not have a monotonic impact on the change in R : small alterations in ω_i , above the threshold, can have the same impact on R as bigger alterations.

region of high sample-to-sample fluctuations is by now fixing the network, and changing the frequency of a single unit by an amount $\delta\omega$. Fig. 1.5(b) illustrates the change δR in the phase synchronization, compared to the synchronization of the "original" ($\delta\omega = 0$) frequency realization. There is a rough threshold, at $|\delta\omega| \gtrsim 0.1$, below which perturbations in one unit do not significantly affect the network's phase synchronization. Above this threshold, however, large changes occur. They are asymmetric on $\delta\omega$ and occur non-monotonically (increasing $|\delta\omega|$ does not necessarily lead to bigger changes). This complicated pattern we observe could make the design and control of these systems quite difficult in practice.

1.3.4 Ratio of short to long-range connections

As we have seen, the rewiring of connections in WS networks, or the redistribution of weights in DD networks, from short-range to long-range connections leads to a transition towards globally phase-synchronized regimes. During these transitions, the dynamical malleability peaks for some ratio of short-range to long-range connections. To quantify

this ratio, we first define the short-range connections to/from a node i as all existing connections to/from other nodes j within an edge distance d (with index $j \in [i-d, i+d]$), with d being the range of short connections ($d = 2$ here). For WS networks, we calculate the average degree (number of connections) for short-range (K_s) and long-range connections (K_l). For DD networks, we define an analogous measure of topological influence, which is:

$$K_s := \frac{2}{\eta(\alpha)} \sum_{j=1}^d \frac{1}{j^\alpha} \quad (1.4)$$

$$K_l := \frac{2}{\eta(\alpha)} \sum_{j=d+1}^{N'} \frac{1}{j^\alpha}. \quad (1.5)$$

Note that due to the symmetry of the DD networks, nodes share the same value of K_s and of K_l . The ratio κ of short-range to long-range connections is then defined as:

$$\kappa := \frac{K_s - K_l}{K_s + K_l}, \quad (1.6)$$

so that $\kappa = 1$ if only short-range connections exist, and $\kappa = -1$ if only long-range connections exist, with intermediate cases in between. In WS networks, the number of connections is $K = kN$ (k being the amount of neighbors of each node), with the number of long connections approximately $K_l = pK$ and short-range approximately $K_s = (1-p)K$. Therefore, the ratio κ can be easily calculated to be approximately $\kappa = 1 - 2p$. For DD networks, the ratio κ is given as

$$\kappa = \frac{\sum_{i=1}^d i^{-\alpha} - \sum_{i=d+1}^{N'} i^{-\alpha}}{\sum_{i=1}^{N'} i^{-\alpha}}. \quad (1.7)$$

Figure 1.6 shows this ratio κ calculated for the same setup of Fig. 1.3(e) and (f), shuffling natural frequencies with fixed coupling strength and changing p or α . The dynamical malleability is measured here by standard deviation χ across the samples, instead of Δ . The former makes the figure clearer, but the same analysis also works using Δ . A remark when comparing with Fig. 1.3 is that the two measures may peak at slightly different values of p or α . For both types of networks, the malleability peaks when there is a relatively small number of long-range connections present in a short-range-dominated network. It is more extreme for WS, as the ratios are closer to 1 than in the DD networks. This discrepancy in the ratios leading to higher malleability shows that κ is not an universal feature for any topology, but can still be important to understand their behavior.

1.3.5 Multistability

So far, we have changed natural frequencies while keeping initial conditions fixed. Now we invert this, and shuffle initial conditions to study the system's multistability. We continue examining phase synchronization (PS) R , although we know that R is only a rough measure of multistability. Being a mean value, the same R could represent different attractors. Therefore, the number of attractors estimated based on R can only be considered as a lower bound. To remedy this, we also verified the findings by comparing several other features of the dynamics. These included the standard

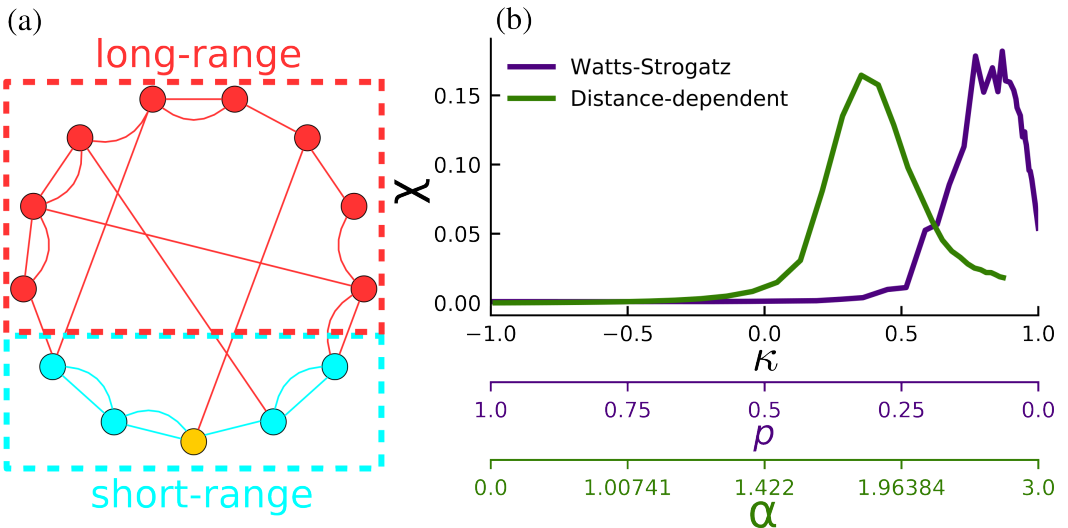


Figure 1.6: Dynamical malleability peaks within a narrow interval in the relation of short-range to long-range connections. Panel (a) illustrates the short-range (blue) and long-range (red) connections from the yellow unit for $d = 2$. Panel (b) shows the sample-to-sample fluctuations in the phase synchronization measured as the standard deviation χ of the distribution function of R against the ratio κ of short-range to long-range connections calculated for several distinct topologies p and α . The green curve corresponds to the distance-dependent networks, with $\epsilon = 6.46154$ and 501 realizations per α ; purple corresponds to Watts-Strogatz networks, $\epsilon = 4.51282$ and 1501 realizations per p . The bottom axis show the values of p and α for the respective ticks in κ (note that values of α are not equally spaced).

deviation of PS in time, the PS between each unit and its neighbors, the PS between sections of 100 units, the time-averaged instantaneous frequencies $\dot{\theta}_i$ of units, and the standard deviation, inter-quartile interval and gap between the unit's instantaneous frequencies. Realizations with unique values of all these features were considered as a distinct attractor. The number of such attractors agrees qualitatively with the dispersion we see in R , increasing during the transition.

The phase synchronization is thus shown in Fig. 1.7. Random networks ($p = 1$, red) seem to be multistable only during their transition to phase synchronization, but this could be a numerical difficulty due to long transients. Intermediate networks ($p = 0.19684$, green; $p = 0.08733$, purple) have a high degree of multistability, meaning coexistence of several attractors, with very distinct degrees of phase synchronization. No shuffle of the initial conditions leads here to the same attractor, so the system has at least 501 attractors, the number of different realizations tested. The 2-nearest-neighbor lattice has significant multistability for $\epsilon \gtrsim 4$. This is consistent with the literature for 1-nearest-neighbors, in which multistability occurs after the transition to phase-locking [51].

To investigate further the multistability, we switch briefly to a smaller network with $N = 100$ nodes to facilitate the multistability analysis. We use the featurizing method introduced in Sec. ???. We have used the phase differences between the units as features for identifying the attractors, and performed extensive testing to ensure this works correctly. In particular, we compared these features with other well-known features, previously

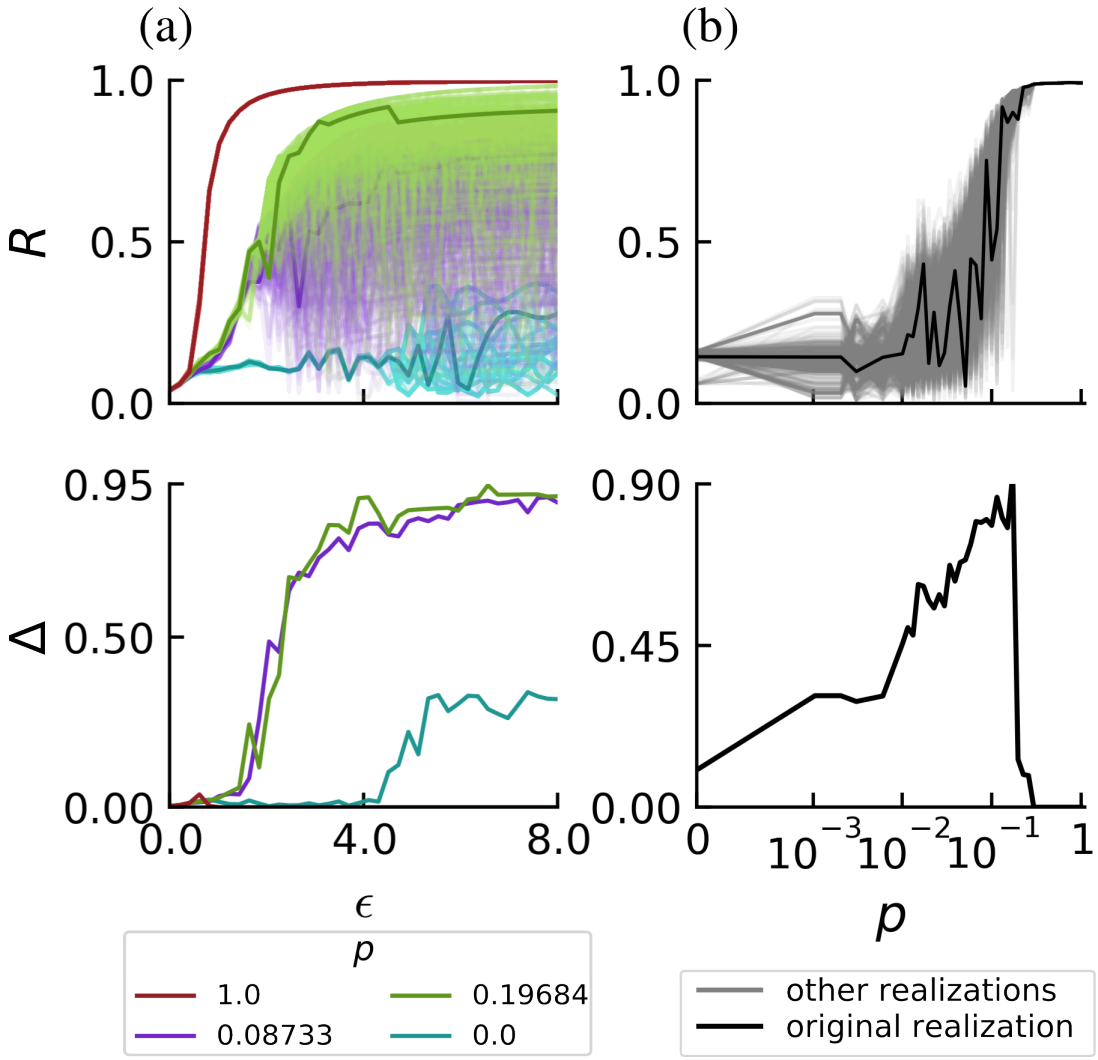


Figure 1.7: **Multistability in WS networks.** Phase synchronization and its dispersion for 501 different shuffles (thinner lines) of the initial conditions, taken from the original initial conditions (thicker lines) used throughout the rest of this work. All other parameters are fixed, including the natural frequencies as the original frequency distribution. The coupling strength ϵ (left panel) and rewiring probabilities p (right panel) are the same ones used for WS networks in Fig. 1.3. The multistable behavior is thus very similar to what we observed before by changing the frequencies (Fig. 1.3(a) and (e)), and so shuffling the initial conditions for this network also leads to large fluctuations in the phase synchronization.

described, such as the network's global degree of phase synchronization and local degree of phase synchronization. The results were identical, and no attractor seemed to be missed. Further, we verified that the number of initial conditions used was enough, and that increasing the simulation or transient time did not alter the results. The attractors are identified in a continuation scenario, where previously found attractors are sampled and added to the pool of initial conditions used for the subsequent parameter. To match the attractors across parameters, the basin enclosure matching method proved to work

best after extensive testing. This was also described Sec. ??.

We start analyzing a network with $p = 1.0$. For sufficiently long transient times, the algorithm finds only one attractor in state space for each coupling strength ϵ . In Fig. 1.8 we show three distinct networks, each with a different shuffle of the natural frequencies. We see that the attractor of all networks has a transition to phase synchronization as ϵ increases. The very beginning of the transition is similar, and the very end is also similar. However, in the middle, during the transitions, the differences between the networks become large, since each network starts their transition at different ϵ . In this region where each network is different, switching from one network to the other (e.g., by shuffling the natural frequencies) brings the trajectories from one attractor that is highly synchronized to another that is still desynchronized, for instance. This corresponds to the increase in sample-to-sample fluctuations near phase transitions in finite networks.

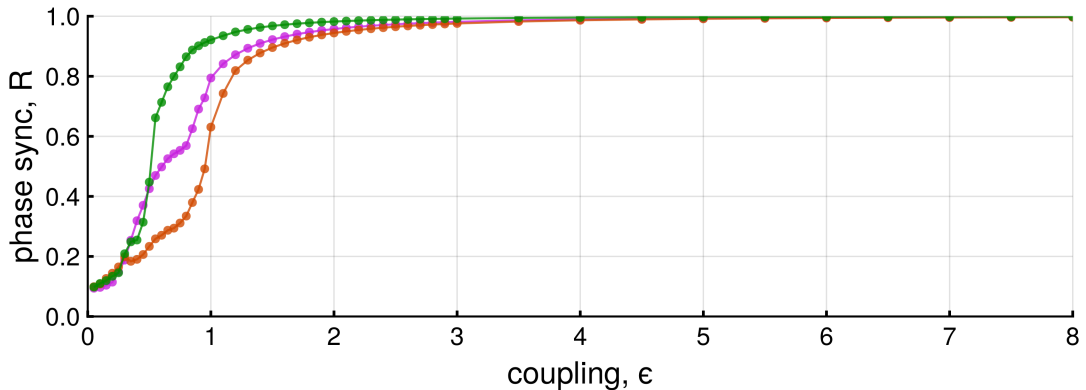


Figure 1.8: **Multistability in random networks with $N = 100$.** Each color in this figure corresponds to the single attractor existing across ϵ for different shuffles of the natural frequencies, with the topology fixed at $N = 100$ and $p = 1.0$. Only one attractor is found for each value of ϵ . These random networks therefore seem to be monostable. However, they are still malleable, as the different shuffles transition to phase synchronization at different coupling strengths ϵ , leading to sample-to-sample fluctuations.

The random networks therefore do not seem to be multistable. If we now switch to small-world networks we see the emergence of many attractors. Figure 1.9 shows the identified attractors for one realization of the natural frequencies - meaning only the coupling strength is changed across simulations. The top panel again shows the degree of phase synchronization of the identified attractors. We see that the initial attractor, in purple, present for small ϵ remains as ϵ is increased. And more attractors eventually appear in the system. One such attractor, in gray, eventually becomes the most synchronized attractor (MSA). The basin of attraction of the MSA also seems to dominate the state space, as shown in the bottom panel, where the fraction of initial conditions converging to each attractor is shown. The MSA already emerges with a large basin of attraction. Interestingly, the size of the basins vary considerably across attractors, suggesting a rich organization of the basins in state space. This analysis uncovers the rich multistability in these systems, and confirms the results we obtained previously for the $N = 501$ networks. It does not immediately reveal the bifurcations

giving rise to the attractors, and does not provide information about the structures of their basins of attraction. Further work is needed in the future to better understand this.

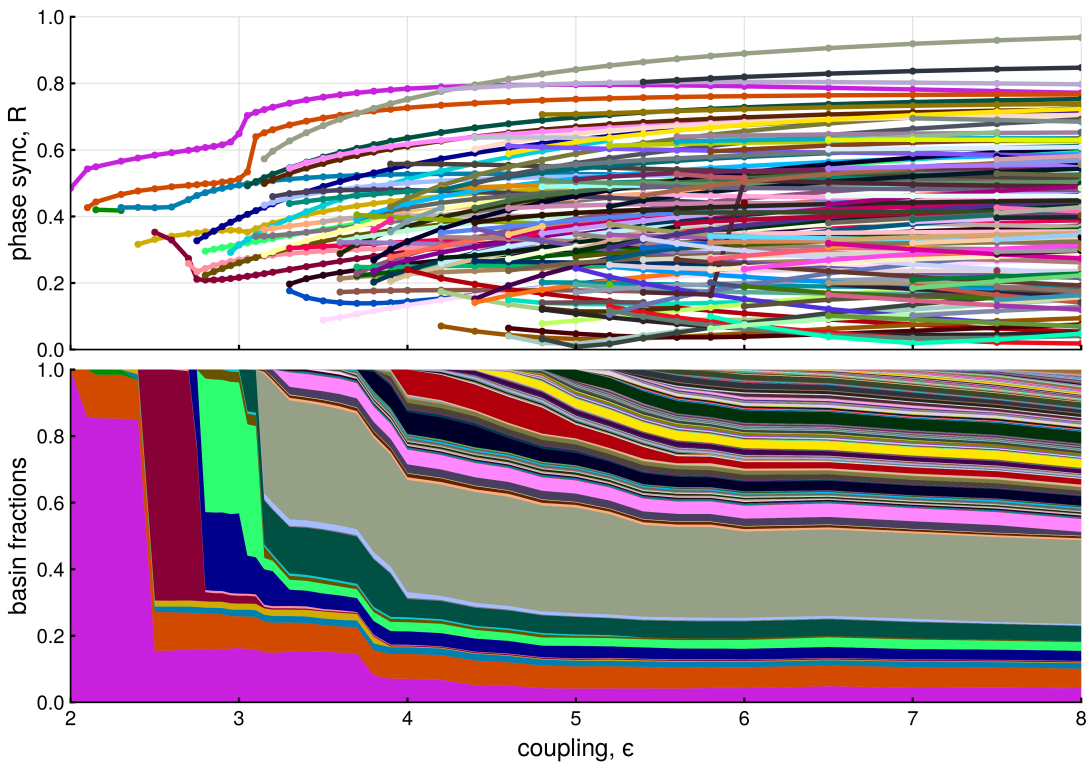


Figure 1.9: Multistability in a small-world network with $N = 100$. The network is fixed, including the natural frequencies and topology with $N = 100$ and $p = 0.08$. Each color in this figure corresponds to an attractor, matched across different ϵ . The top panel shows the time-averaged degree of phase synchronization R while the bottom panel shows the fraction initial conditions converging to each attractor for each ϵ . A rich multistability is therefore observed, with attractors having differently sized basins of attractor, as ϵ becomes sufficiently large. The gray attractor exhibits a typical transition to phase synchronization, but other attractors do not necessarily. The analysis was done using the featurizing and continuation algorithms described in Sec. ??.

The multistability can enhance the sensitivity of the networks to parameter changes, and helps to explain the large fluctuations we observe. In this case, a parameter change needs only to change the boundaries of the basins of attraction for the same initial condition to land on a completely different attractor. Attractors do not have to be necessarily drastically changed for the large dynamical malleability to be observed. However, multistability is not in principle required for STS fluctuations; in fact, the random and the distance-dependent networks appear to be monostable (not shown), though they are malleable.

1.3.6 Distributions of samples

As we have seen, shuffling initial conditions can also generate realizations with widely different dynamics, similarly to shuffling natural frequencies. But the two methods to create an ensemble of samples have different effects, and can generate samples with distinct distributions. As shown in Fig. 1.10 for Watts-Strogatz networks, shuffling frequencies leads usually to a broader, and smoother, distribution of R . This increased broadness shows that new attractors are indeed created by shuffling the frequencies, so that multistability itself cannot account for the dynamical malleability we discussed previously. Furthermore, the transitions to phase synchronization occur through an increase in the distribution's average. The accompanying increase in the width of the distribution shows an increase in dynamical malleability, which goes to zero only for long-range networks ($p = 1$).

Specifically, the distributions for the two-nearest-neighbor lattice ($p = 0$, panels (a)-(e)) are quite different: shuffling frequencies leads to a smooth distribution, whose average shifts to the right as ϵ is increased; for shuffling initial conditions there is also a slight increase in the distribution's average as ϵ is increased, but the distribution itself is dominated by several peaks. For intermediate networks ($p = 0.08733$ and $p = 0.19684$, panels (f)-(o)), the skewness of the distribution becomes negative, and shuffling initial conditions has a smoother behavior, more similar to shuffling frequencies. Interestingly, the distribution can be bi-modal, with the two modes being separated on either extreme of R (panels (n) and (o)). For $p = 1$ (random network), the two first coupling strengths (panels (p)-(q)) occur during the narrow interval of significant malleability, during the transition to phase synchronization. Soon after $\epsilon > \epsilon_c \approx 1.6$, the distribution becomes extremely narrow.

It is worth mentioning that very similar distributions are obtained if, instead of shuffling the frequencies or initial conditions, we re-sample them from the distribution (i.e. change the seed in the random number generator). Interestingly, the distributions are not Gaussian, which is inconsistent with the assumptions made in other works [46, 38]. In these works, the authors argue that the fluctuations must be normally distributed for sufficiently large networks and many samples due to the central limit theorem. This inconsistency is likely generated by the finite size of the networks studied here. Even in all-to-all networks, in which there is no topological disorder, the distributions are not Gaussian for $N = 501$. Results (not shown) indicate that the distributions approach Gaussian distributions as N is increased to 5000.

1.4 Discussions and conclusions

Summary

In this work, we have studied the sensitivity of networks to changes in their units' parameters or connections, which we call their dynamical malleability, and showed that, near transitions to phase synchronization, this behavior acquires (i) a large magnitude, as changes to single units can radically alter the spatiotemporal dynamics, and (ii) a complicated sensitivity, as no analytical method we have tried was able to satisfactorily describe the changes to the dynamics. Parts of this behavior have been observed in isolation previously [11, 33, 27, 32, 34, 35] but this is, to the best of our knowledge, the first work to focus specifically on it and show its full phenomenology.

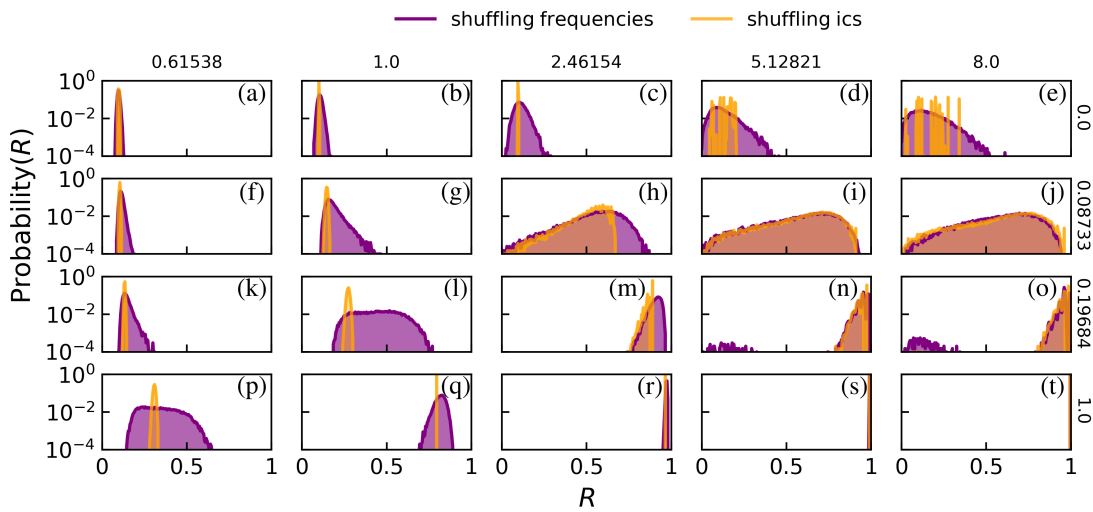


Figure 1.10: Distributions of R due to shuffling frequencies or initial conditions. Each panel contains the distribution of the mean degree of phase synchronization R across 20000 shuffles of natural frequencies (in purple) or initial conditions (orange) for Watts-Strogatz networks. The rewiring probabilities p are indicated on the right of each row, and are the same as used in Fig. 1.3(a); the coupling strengths ϵ are indicated on the top of each column. Bin size is 0.005, and the probability for each bin is calculated as the occupation of the bin divided by the total occupation across all bins, and is shown in logarithmic scale.

To study this concretely, we have chosen ring networks of Kuramoto phase oscillators and connected the units in two distinct classes of topology, Watts-Strogatz (WS) and distance-dependent (DD). We have either changed the frequency of a single unit or changed the frequencies of all units by shuffling (i.e., redistributing) the values of the frequencies across units. The first has allowed us to verify the impact of relatively small changes, which are still not small enough to be described in the linear regime; the latter allowed us to verify the impact of redistributing the values in the network while keeping the distribution of parameters exactly the same, which is helpful for identifying mechanisms for the fluctuations.

Mechanisms for dynamical malleability

The two classes of topology we used have different characteristics (see Sec. 1.2) but are similar in that they lead to networks that have two distinct types of transition to phase synchronization: one induced by increasing the coupling strength and another by increasing the dominance of long-range connections. They also have differences, mostly notably that (i) the WS networks acquire a large number of attractors during their transitions to phase synchronization (i.e. become highly multistable), while the DD networks remain with one main attractor (and possibly other attractors that would have very small basins of attraction), and that (ii) the WS networks have a larger magnitude of dynamical malleability. We believe that this larger magnitude is caused by two effects: the increased number of attractors and the topology's link-disorder.

Firstly, we remark that the dynamical malleability is manifested in the networks'

transitions to phase synchronization in two distinct ways. The first is through diverse onsets of the transition, as different realizations start their transitions at different values of the control parameter. This is the well-known blurriness of phase transitions described in studies of finite-size effects [49, 52]. This effect is clearly present in both networks (see, e.g., Fig. 1.3(a) and (b)). The second manifestation of malleability is in the post-transition fluctuations, i.e., in the sudden changes of synchronization that occur after the network has seemingly transitioned to synchronization (see, e.g. Figs. 1.3(a) and (c)). This effect is present here mostly in the WS networks, but is also known in other systems of finite size (see, e.g. Figs. S5(b) and (d) for the case of cellular automata). It is caused at least partly by the system's multistability, as increasing the parameter can change the shape of the attractors' basins of attraction, making the same initial condition suddenly go to another attractor. So the WS networks, which have a much larger number of attractors, exhibit this additional effect that increases their malleability, while the DD networks do not.

We further remark that multistability could have an even more pronounced impact on malleability if the basins of attraction were complexly interwoven. Then, even very small changes could lead to significant fluctuations. But this does not appear to be the case in any of the networks we studied, all of which seem to have smooth basin boundaries (Fig. S4) - it is thus noteworthy that the already high dynamical malleability we have described can occur even with smooth basin boundaries. It can even occur in the absence of multistability, as seen in the DD networks.

The second mechanism for the increased malleability in WS networks is their link-disorder [38]: different realizations lead to different topologies for a same parameter, and we observe a very similar phenomenology by comparing different realizations of these topologies (Fig. S1). This is a source of disorder, and thus, of fluctuations, that is not present in the DD networks.

Mechanisms for the fluctuations

As we have mentioned, the fluctuations in the malleable networks are also hard to predict. The behavior of the systems is clearly a complicated function that involves the coupling strength, topology, natural frequencies, and initial conditions all together. For instance, we have not found a sequence of frequencies, or a specific network realization, that always leads to more (or less) synchronized networks (Fig. 1.5(a)). Even for fixed frequencies and topology, the most phase synchronized realization changes depend on the initial condition or the coupling strength. Changes in the natural frequency of single units also lead to non-monotonic changes in the network's phase synchronization: the change in frequency can either increase or decrease the synchronization level, depending on the chosen unit, coupling strength, and topology (Fig. 1.5(b)).

As a consequence, we are unable to identify a specific unit, or magnitude of perturbation, that is always responsible for the greatest disruption. That is, no available theory in the literature that we have tried revealed a mechanism for the fluctuations capable of predicting them. This is a surprising result, considering the quality of the available theories, the amount of research and important advancements in the description of networks similar to the ones studied here [32, 53, 54, 55]. We believe that this is mainly caused by the networks' multistability, which cannot be handled by some theories, and by the wide range of synchronization patterns.

The first theory we tried is the synchrony alignment function, which depends on

the topology and natural frequencies and was shown analytically to be related to the degree of phase synchronization in the limit of strong synchrony [53]. It does not work satisfactorily for any dynamically malleable network that we tested. One reason for this is the weak phase synchronization in some realizations, which breaks the assumption of the method. Another, even stronger, reason is that our networks are multistable, such that the relation between the synchrony alignment function and the degree of phase synchronization given by the method cannot be satisfied for all attractors of the system. Indeed, it only worked perfectly in the strongly phase synchronized regime, which is also monostable.

The second theory we tried is due to Peter and Pikovsky [32], who showed in all-to-all networks that different realizations of the natural frequencies synchronize differently depending on the kurtosis of the distribution. This mechanism cannot even be expected to work for the shuffling scenarios we study since they conserve the frequency distributions and thus the kurtosis as well, but we have verified that it also does not work when the units' frequencies are changed. An additional reason why this does not seem to apply in our systems may be in the topologies, which are not all-to-all.

Thirdly, we have tested other measures that have been observed in the literature to correlate to phase synchronization, and they do not work in the malleable networks. These are: (i) the proportion p_- of links connecting nodes with natural frequencies of different signs [54]; (ii) the correlation c_ω between the oscillators' natural frequencies, taking into account the connectivity of the network [54, 55]; (iii) the correlation between natural frequencies and the node's number of connections [53]; and (iv) the correlation between the average frequency between neighbors of a node and the node's own frequency [56, 53]. These results also cannot be expected to work in multistable networks, and indeed did not work in our networks.

Relation to statistical physics and scaling

As noted previously, there is a relation between our dynamical study here and studies on the statistical physics of networks. The transitions to phase synchronization that we see correspond to non-equilibrium phase transitions [36, 32], such that we can connect the dynamical malleability we analyze with the well-known sample-to-sample (STS) fluctuations in statistical physics. These are usually described in finite systems, in which different samples have different statistical properties that lead to distinct phase transitions - the transitions are usually said to be shifted between samples [57, 58, 46], which is one of the mechanisms we described for the malleability. As seen in these studies, the size N of the system (i.e. the number of nodes) influences the magnitude of the dynamical malleability as well as the interval of parameters in which it occurs. The networks we have presented in the results have $N = 501$ oscillators, and scaling analysis (Fig. S2) reveals that the intervals of high malleability decrease with the size N , as expected from other studies. For instance, authors in [46] describe the range of ϵ for high malleability as scaling with $N^{-2/5}$ for all-to-all networks.

For the WS networks, malleability is still significant for even up $N = 5000$ oscillators. Moreover, the maximum magnitude of the fluctuations does not decrease significantly, and networks with $N = 5000$ can still reach $\Delta = 0.9$. This suggests that the malleability gets restricted to a smaller region in parameter space, but might not decrease significantly in magnitude for bigger networks. In the limit of infinite-size networks, it would get restricted to a single line, defining the two types of transitions to phase synchronization,

and remain non-zero there. This is consistent with a study in all-to-all networks of Kuramoto oscillators, where this behavior was observed [47]. In fact, this behavior is well-known for phase transitions with quenched disorder (heterogeneous parameters), when systems are said to be non-self-averaging [59]. In any case, networks of $N = 5000$ units can be regarded as rather large in several real-world applications [32], so the STS fluctuations we describe here occur for a significant range of system sizes.

Generality of the behavior

Additionally, we show that the increase in dynamical malleability is widespread in the parameter space of the systems. Looking at this space, spanned by coupling strength and the parameter controlling the topology, the dynamical malleability remains high over a wide parameter range around the two types of transitions to phase synchronization. In particular, networks with an intermediate amount of long-range connections are highly malleable for any coupling strength ϵ we tested (e.g. green and purple lines in Fig. 1.3). This is because the topology is fixed, so the networks remain close to the topology-induced-transition even though they are far from the coupling-strength-induced-transition.

We also remark that the phenomenology we describe also occurs for wide ranges of topology and coupling strength values, for distinct frequency distributions, such as Cauchy-Lorenz (not shown), and for other dynamical models. For instance, previous works on spiking [11] and bursting [35] neural networks have revealed a very similar phenomenology. We also show similar behavior for cellular automata (see Fig. S5). We have observed (not shown) similar behavior in small-world networks generated by adding long-range connections and keeping the short-range ones [60]. Other works have also observed dynamical malleability in Kuramoto oscillators coupled under both human-connectome structural networks and hierarchical-modular networks [61, 62]. Additionally, of course, the theory of phase transitions and, consequently, of sample-to-sample fluctuations is known to apply for a variety of distinct systems.

Practical importance of malleability

The discussions lead to an interesting question: is dynamical malleability good or bad? On the one hand, large fluctuations can be undesired. For instance, a large fluctuation could take power grids from a phase synchronized regime to a desynchronized one, and lead to blackouts. On the other hand, fluctuations can be desired due to the increased flexibility in the systems. They could be a useful mechanism for adaptation, learning or memory formation in neural circuits. More specifically, an important property of the brain is that it can separately process information from different types of input in segregated areas, and then integrate them all into a unified representation [63, 64, 65]. For this reason, Tononi and colleagues conjectured that the brain needs to have an optimal balance between segregation and integration of areas [63]. In this optimal balance, the synchronization between different brain regions needs to fluctuate from low synchronization to high synchronization [66]. Therefore, having a large dynamical malleability can be an advantageous feature, allowing for this high variability to be achieved through small changes in the neurons, e.g. their firing rate, or their connections. There is also interesting evidence for this in [67], which reported that high-frequency firing of neurons can drive changes in the global brain state.

Future research and conclusions

An interesting line of research opened here is to understand ways to quench or to explore the fluctuations between realizations, using the framework we establish here, for practical applications. Another interesting line of research is to consider the effects of noise or time-dependent forcing on malleable systems: since they have a wider range of dynamical states available by changing parameters, a time-dependent change in the parameters, induced by the noise or forcing, can lead to transitions between several different states. The complicated and sensitive dependence on the parameters would mean that even small amplitude changes could lead to drastic fluctuations. For the Watts-Strogatz networks, multistability can complicate the dependence on external inputs, and make the effects dependent on the timing of perturbations, as different states, all of which coexist, can react differently to the parameter changes. Understanding these behaviors is important, for instance, in the context of neural systems, where external influences are common and where temporal fluctuations are essential.

Future research is also needed to fully describe the mechanism for the fluctuations between realizations. An interesting possibility could be to extend the synchrony alignment function [53] to weakly synchronized regimes or to multistable systems. Another promising approach would also be to apply the formalism introduced in [68, 69]. A third possibility would also be to use the model reduction method by [70]. These would be important theoretical contributions for the understanding of phase synchronization in oscillator networks and for the role of each unit in a network.

To summarize, the increased magnitude and complexity of dynamical malleability shown here is a general phenomenon in finite-size systems that can be expected to occur in real-world systems.

Acknowledgments

We would like to thank Jan Freund and Arkady Pikovsky for helpful discussions. K.L.R. was supported by the German Academic Exchange Service (DAAD). R.C.B. and L.E.M. acknowledge the support by BrainsCAN at Western University through the Canada First Research Excellence Fund (CFREF), the NSF through a NeuroNex award (#2015276), SPIRITS 2020 of Kyoto University, Compute Ontario (computeontario.ca), Compute Canada (computecanada.ca), and the Western Academy for Advanced Research. R.C.B. gratefully acknowledges the Western Institute for Neuroscience Clinical Research Postdoctoral Fellowship. B. R. R. B. acknowledges the financial support of the São Paulo Research Foundation (FAPESP, Brazil) Grants Nos. 2018/03211-6 and 2021/09839-0. The simulations were performed at the HPC Cluster CARL, located at the University of Oldenburg (Germany) and funded by the DFG through its Major Research Instrumentation Program (INST 184/157-1 FUGG) and the Ministry of Science and Culture (MWK) of the Lower Saxony State, Germany.

Chapter 2

Conclusions

Science is typically reductionist [71]. We break a hard problem into smaller parts that are easier to understand separately. We have achieved tremendous success with this effort, but we have not solved everything; indeed, we have found out that putting everything back together can be quite complicated: the interactions between the parts can generate complex behavior that is not present in any one of the parts alone. The field of complex systems arose from the need to understand this *emergent phenomena* - to (re)construct the full system's behavior from knowledge of its parts. In the case of networked systems, studied in this thesis, the challenge can be phrased as the need to understand how the whole system's behavior arises from the coupling between the units. A major challenge still today is to develop tools that allows us to characterize and understand complicated emergent behavior.

One such complicated behavior in networks is the coexistence of multiple stable solutions to the same equations with the same parameters - *multistability*! How do these solutions come about, where they are situated and how they are separated in state space - these are all questions under active research [72, 73, 29].

Some of these stable solutions may correspond to synchronized regimes, which brings into light another important phenomenon: *synchronization*. Here again the field of complex systems has to contend with another problem: how individually distinct units can cooperate together and start to operate in unison, in a beautiful example of an emergent phenomenon. The study of synchronization - both frequency and phase synchronization - also has important practical motivations, for instance in the study of power grids. In power grids, and other complex networks, understanding the robustness of solutions, in particular of synchronized solutions has been an object of active research.

Combining these two research areas, Chapter 1 investigated the robustness of solutions in a complex network of Kuramoto oscillators, a paradigmatic model for studies on synchronization phenomena and complex networks in general. The idea was to investigate how the network behaves - how the solutions change - when we alter the parameter of a single unit in the network. We found that the *dynamical malleability* of the network depends on how strongly coupled the units are, and the topology of the connections. Roughly, we showed that for very weak coupling strength the individual tendencies of the oscillators win and most of them oscillate incoherently. For sufficiently strong coupling, most of the oscillators become phase locked - they oscillate at the same frequency. This is the same behavior as in all-to-all networks (see Sec.??). The spatial pattern of the phases, which we can measure via the degree of phase synchronization, was then determined by the topology. For several of the coexisting attractors, including the most phase synchronized attractor, the following tendency was observed: networks dominated by short-range connections tend to have attractors with short-range patterns (phase desynchronized), while networks dominated by long-range connections tend to have attractors with long-range patterns (phase synchronized). In parameter space, phase synchronization in these networks lives in the region of sufficiently high coupling strength and number of long-range connections. Changing the parameters toward this region therefore makes the system undergo a transition to phase synchronization. We showed that precisely during this transition their dynamical malleability increases con-

siderably. To the point that changing a single unit radically alters the pattern of phases in the network, potentially changing it from phase synchronized to phase desynchronized.

The mechanism for this dynamical malleability is two-fold. First, it is related to *increased sample-to-sample fluctuations* near a phase transition [46, 58]. This mechanism does not require multistability. In fact, suppose the systems have a single attractor, like the randomly connected networks. Each change to a parameter of a unit leads to a different dynamical system, which may have a different attractor. In particular, the transition to phase synchronization of this attractor may occur at different coupling strength values, earlier or later compared to the system before the change. If we enact this change but keep the coupling strength fixed, we switch to an attractor that has a smaller or larger value of phase synchronization - this is the fluctuation from one sample to another. If the systems have multiple attractors, this effect is still there, but there is the added possibility of switching to other attractors, which might be even more different. The *multistability* increases the possible fluctuations that may occur. This explains our observation that for Watts-Strogatz networks the malleability and multistability seem to go hand in hand. It also explains why these networks have a considerably larger malleability than the distance-dependent networks, which do not seem to be multistable.

An important concept in the area of complex systems is that of global stability, typically taken to mean the relative size of the basin of attraction of each attractor. In this view, attractors whose basins occupy larger regions of state space are more globally stable [74]. The rough idea is that trajectories on attractors with bigger basins of attraction are more likely to require bigger perturbations in order to be kicked across the basin boundary and into another attractor. This is not necessarily the case, however, since the situation depends on the geometry of the basin of attraction [75], but it highlights the importance of studying perturbations applied to the state of a system. In general, more attractors means they are sharing state space more and therefore the global stability is smaller, meaning the system is less robust (or less resilient, depending on terminology [75]). In this work we show that multistability affects the robustness of the system in another way: by affecting its malleability. So not only is it dangerous to kick the state of the system, it is also dangerous to change its parameters - even the parameter of one single unit!

Another important observation was the study of how malleability, and multistability, depend on the topology of the system. Topologies that put the systems in the vicinity of a transition to phase synchronization, which were in the small-world range, made it very malleable. An important question that is left for future work is why these specific topologies lead to a higher number of attractors - which properties do they possess that lead to the emergence of the attractors, compared to, say, the random topologies, which do not induce multistability? The distance-dependent networks also do not seem to be multistable, a factor that would also be interesting to investigate.

A related question is about the generality of these results. Malleability due to sample-to-sample fluctuations is very common, being extensibly described in statistical physics literature [57]. We also described it initially in a network of spiking neurons [11], and observed it in the Kuramoto model under different topologies of distributions of the natural frequency, and under other models, such as a simple model of excitable cells. We believe that the multistability results will also generalize somehow - supported by the available evidence from other works - but this is also object of future research. Understanding better the mechanisms generating the multistability will also help answer

this.

In a similar vein, we also investigated how multistability emerges when excitable neurons are coupled diffusively. Excitability in the individual units here occurs due to the presence of a saddle and an unstable equilibrium in state space, which force part of the trajectories to go around on a long excursion before eventually converging to the stable equilibrium. These region where trajectories go through is called the *excitability region*. We showed that the coupling can trap trajectories in this excitability region by repeatedly reinjecting them there. This mechanism underlies all the emergent attractors we observed, even though they arise due to different bifurcations: saddle-node of limit cycles and homoclinic. For two units, it can create three coexisting periodic attractors, and can also create a quasiperiodic attractor. For more units, it can create a larger number of attractors, including potentially a chaotic attractor. Based on the trapping mechanism and preliminary results, we conjecture that the topology of the networks plays a key role in dictating which attractors emerge, and how many. This could be very similar to Kuramoto networks, and a more in-depth comparison is definitely warranted. It would be very interesting in the future to explore how exactly the size and topology of the networks control the emerging attractors.

In this initial work we decided to focus mainly on the pure dynamics of the system, so we showed most of the results in the case where the coupling is applied to both the x and y directions of the system. In some models, such as ecological models - where the diffusive term would model a migration of species - this might be very sound. For the neuronal case, however, only the x -coupling is biophysically sound. Motivated by this fact, we also investigated how the attractors change when the coupling is applied to only one variable. Interestingly, the mechanism is still present, but the two main types of attractors we observed split up when the coupling is split. The exclusive x -coupling leads to the attractor with two units trapped in the excitability region (LA-LA); the exclusive y -coupling leads to the one with only one unit in the excitability region (LA-SA or SA-LA). We confirmed this with a bifurcation analysis and also qualitatively explained it based on the geometry of the attractors and the trapping mechanism. This is important in terms of potential applications. First, it means that adding a gap junction between two otherwise silent neurons could make them bistable, with the possibility of periodic or even quasiperiodic spiking. In fact, there is some evidence that this seems to occur in neurons coupled under gap junctions in the motor cortex of fruit flies [76]. It is also interesting in the ecological direction, if we consider that only some species in an ecological niche might be migrating between patches.

Furthermore, we focused for simplicity on the excitable case, where the trapping mechanism creating the attractors is more easily seen. But attractors still emerge similarly in a bistable regime, where the stable equilibrium coexists with a stable limit cycle. We can achieve this by changing the input current I of the model. A difference in this case is that the uncoupled neuron already has an oscillating attractor. Therefore, when they are diffusively coupled they can also synchronize together in this oscillating attractor. This system thus has the possibility of achieving full synchronization on a periodic attractor. In this case, one could reframe the study in terms of the stability, global and linear, of the synchronized state, and how the coupling might create new attractors and thus reduce the relative size of the basin of the synchronized attractor.

We initially arrived at this problem when trying to understand the synchronization behavior of a network of bursting neurons [77]. The degree of phase synchronization in that system changes nonmonotonically as a function of the coupling strength: increas-

ing the coupling initially increases the phase synchronization, then actually decreases it in a certain region, before increasing it again for very strong coupling. This is also reminiscent of a behavior observed in networks with chaotic saddles in Ref. [78]. We also studied a network of bursting neurons following another model, and found that a chaotic saddle was important there but also a slow region of system's limit cycle was related to the multistability that emerged. From the work on excitable neurons, we understand that slowness can help generate attractors, at least for the reinjection mechanism we observed. It would be interesting in the future to go back and finish the initial studies.

When working on a project, I believe it is not an uncommon feeling to find an interesting paper, try to replicate its results and not quite manage. Then, to look at the source code that the authors hopefully provided, and to be underwhelmed. While working on a paper, it is often the case that people might want spend as little time as possible implementing the algorithms they need, leading usually to confusing code, which might not be as efficient as it could, and not as well-tested - and thus, more susceptible to errors. One solution to this is to create a unified library that implements efficient code, tests and documents it. And to make it open-source, to share it with the whole community. Then, anyone can scrutinize the code, find improvements and test it further. Also, more importantly, everyone can use it. This saves implementation time, potentially run times due to improved code efficiency, and also re-implementation time for poor students aiming to replicate papers. This is the philosophy of the dynamical systems library [79], started by Dr. George Datseris, written in the Julia programming language. With this idea in mind, we also collaborated to implement algorithms related to finding attractors and their basins. In particular, I worked on the algorithm used in the two multistability works in this thesis. It is a brute-force algorithm that integrates trajectories, converts them into vectors of features, and selects attractors as unique groups of features [31, 80, 81]. Together with Prof. Alexander Wagemakers, we also implemented an algorithm that applies attractor-finding algorithms across a parameter range, in a continuation manner. The result of this work was the *Attractors.jl* package, also co-developed by more collaborators, and a publication describing this novel algorithm and improvements to previous literature [81].

So far on the study of dynamical systems we have mostly focused on attractors. The motivation for this is that attractors represent a system's long-term dynamics: after some *transient* time, trajectories converge to attractors. There is, however, a key assumption here: that the period of time during which we observe the system T_{obs} is longer than the convergence time T_{conv} to the attractor. It is a matter of time-scales: of the observation versus the relaxation to the attractor. Whether this can be guaranteed or not depends on the application. In power grids, for instance, one is generally interested in the long-term dynamics of the system. In the brain, however, changes may be occurring too fast, and there may not be enough time to wait for convergence to an attractor. The time-scales can also vary within the same system: as we saw in the excitable units, trajectories starting on one side of the state space converge rapidly to the attractor, whereas trajectories starting on the excitability region spend a relatively long time performing an excursion in space before reaching the attractor. This problem is made more complicated due to the fact that there are many mechanisms that can generate long - potentially arbitrarily long - transients. An example is chaotic saddles, wherein trajectories can stay indefinitely long [82]. Therefore, the behavior that is actually observed in some studies may be a transient. Moreover, some of these long-lived transients occur inside attractors. One example can be seen in ghost states

inside chaotic attractors - such as for the Logistic map or the Lorenz system - where the trajectories switch between clearly chaotic and seemingly periodic dynamics (cf. Chap. ??). Another example is the stable heteroclinic cycle: the cycle as a whole can be an attractor, but trajectories on it switch between the neighborhoods of saddle-points, describing sequences of metastable regimes. Yet another example is crawl-by motion, in which a limit cycle is in the proximity of a saddle-point. The region near the saddle-point may have very slow dynamics, and trajectories on the cycle take a long time to pass through (crawl-by) this region [83]. These examples illustrate the intricate relation between multistability - and attractors - and metastability.

Transients can play important roles. A specific example that illustrates the role of sequences of transient states is the Turing machine, the paradigmatic model for *computations* [84, 85]. It is a simple finite state machine with a head that stores a certain state and can read, write, and move along a tape. The tape is subdivided into cells containing symbols (e.g., 0's and 1's). The head represents a modern computer's central processing unit, while the tape represents the memory. Accordingly, the head follows a set of instructions that take the current state, currently read symbol on the tape and outputs the new state, the new symbol it writes on the tape, and the direction it moves. Computations are done by traversing a sequence of such state-symbol combinations. The machine may run forever - it is said to not halt -, in which case the computation is not completed. If the machine does halt, the computation is finished. From this point of view, therefore, the computation is only complete once the machine terminates the previous sequence of states. This sequence can therefore be seen as a type of transient behavior, which is crucial for the computation performed by the machine. This remark is not just an analogy - dynamical systems can be constructed that implement Turing machines [86].

More concretely, in the brain, transients have been shown to play important roles [87, 88]. There is a plethora of observations showing neural activity going through sequences of distinct states, which are all therefore transient [89, 90]. In several cases, these states are long-lived (i.e., metastable). Understanding the exact roles that *metastable regimes* play in neural circuits is crucial to understanding how they perform computations, a central question in neuroscience and also artificial intelligence [91, 92, 93]. Recent work, based on theoretical and experimental results, has shown that ghosts of saddle-node equilibria, which generate long transients, are a particularly important mechanism [91, 94, 95, 88]. It is expected, however, that other mechanisms are also present in circuits. For instance, a wide literature in neuroscience uses attractors to perform computations, and adds external perturbations to induce changes between regimes [96, 93, 90, 97]. It will be important in the future to contrast these two ideas to see the actual roles played by each of them.

To better understand the role of transients on computations in neural circuits, it is therefore important to have both an in-depth as well as a general understanding of metastable dynamics. Under this logic we developed a *general conceptual framework* for metastability, collecting and refining ideas from the neuroscience and dynamical systems literatures. As seen in Chap. ??, we proposed that the main concept behind metastability is that of long-lived transients, and showed many dynamical mechanisms capable of generating it. In the future, one can use this framework to actively compare the different mechanisms, with a view towards experiments - both biological as well as *in silico*, looking to understand how networks perform computations [91].

Besides the metastable regimes themselves, perhaps the actual *sequences* play an

important role. This is the case in the Turing machine, but there is also evidence in biological networks. An important example, already mentioned in the Introduction and in Chap. ??, showed in a series of works that sequences of metastable regimes are elicited when mice are fed tastants [98]. The sequence of regimes is unique to each tastant, suggesting they play an active role in encoding the stimuli [99]. Sequences of metastable regimes have been linked to computations in other experiments also [88, 99, 96]. In this case, a useful concept coming from dynamical systems theory is that of excitable networks by Ashwin and Postlethwaite [100, 101]. They developed methods that allow one to construct systems with prescribed connections between equilibria states. These connections may be spontaneously activated (as in connected ghosts) or via a perturbation (by perturbing across the basin boundary). This is an example of how the theory of dynamical systems is offering many tools and mechanisms that can be used to model and better understand how circuits are actually solving tasks and performing computations. This is an exciting area for future research.

Taking everything together, the field of complex systems is under intense research, with lots of us aiming to develop theory and tools to understand emergent dynamical phenomena like synchronization, the coexistence of multiple long-term solutions and the (transient) path to them. I believe that during my PhD we managed to provide some timely contributions in these directions, but there is still much to be done - with applications being very significant in biology, technology and even climate. I am very excited to help put all these pieces together.

Bibliography

- [1] Adilson E. Motter, Seth A. Myers, Marian Anghel, and Takashi Nishikawa. Spontaneous synchrony in power-grid networks. *Nature Physics*, 9(3):191–197, 2013.
- [2] Jennifer A. Dunne, Richard J. Williams, and Neo D. Martinez. Food-web structure and network theory: The role of connectance and size. *Proceedings of the National Academy of Sciences*, 99(20):12917–12922, 2002.
- [3] Patrick Crotty, Dan Schult, and Ken Segall. Josephson junction simulation of neurons. *Physical Review E*, 82(1):011914, 2010.
- [4] Micha Nixon, Moti Friedman, Eitan Ronen, Asher A. Friesem, Nir Davidson, and Ido Kanter. Synchronized Cluster Formation in Coupled Laser Networks. *Physical Review Letters*, 106(22):223901, 2011.
- [5] F Varela, J P Lachaux, E Rodriguez, and J Martinerie. The brainweb: phase synchronization and large-scale integration. *Nature Reviews Neuroscience*, 2(4):229–239, 2001.
- [6] Dirk Witthaut, Frank Hellmann, Jürgen Kurths, Stefan Kettemann, Hildegard Meyer-Ortmanns, and Marc Timme. Collective nonlinear dynamics and self-organization in decentralized power grids. *Reviews of Modern Physics*, 94(1):015005, 2022.
- [7] Pascal Fries. Rhythms for Cognition: Communication through Coherence. *Neuron*, 88(1):220–235, 2015.
- [8] W Singer. Neuronal synchrony: a versatile code for the definition of relations? *Neuron*, 24(1):49–65, 111, 1999.
- [9] Arkady Pikovsky, Michael Rosenblum, and Jürgen Kurths. *Synchronization: A Universal Concept in Nonlinear Science*, volume 70. Cambridge University Press, 2001.
- [10] Alex Arenas, Albert Díaz-Guilera, Jurgen Kurths, Yamir Moreno, and Changsong Zhou. Synchronization in complex networks. *Physics Reports*, 469(3):93–153, 2008.
- [11] R. C. Budzinski, K. L. Rossi, B. R. R. Boaretto, T. L. Prado, and S. R. Lopes. Synchronization malleability in neural networks under a distance-dependent coupling. *Physical Review Research*, 2(4):043309, 2020.
- [12] Yoshiki Kuramoto. Self-entrainment of a population of coupled non-linear oscillators. *International Symposium on Mathematical Problems in Theoretical Physics. Lecture Notes in Physics*, 39:420–422, 1975.
- [13] Juan A. Acebrón, L. L. Bonilla, Conrad J. Pérez Vicente, Félix Ritort, and Renato Spigler. The Kuramoto model: A simple paradigm for synchronization phenomena. *Reviews of Modern Physics*, 77(1):137–185, 2005.
- [14] Francisco A. Rodrigues, Thomas K.D.M. Peron, Peng Ji, and Jürgen Kurths. The Kuramoto model in complex networks. *Physics Reports*, 610:1–98, 2016.

- [15] Adrián Ponce-Alvarez, Gustavo Deco, Patric Hagmann, Gian Luca Romani, Dante Mantini, and Maurizio Corbetta. Resting-State Temporal Synchronization Networks Emerge from Connectivity Topology and Heterogeneity. *PLOS Computational Biology*, 11(2):e1004100, 2015.
- [16] Joana Cabral, Etienne Hugues, Olaf Sporns, and Gustavo Deco. Role of local network oscillations in resting-state functional connectivity. *Neuroimage*, 57(1):130–139, 2011.
- [17] B. D. Josephson. Coupled Superconductors. *Reviews of Modern Physics*, 36(1):216–220, 1964.
- [18] Milos Marek and Ivan Stuchl. Synchronization in two interacting oscillatory systems. *Biophysical Chemistry*, 3(3):241–248, 1975.
- [19] John C. Neu. Chemical Waves and the Diffusive Coupling of Limit Cycle Oscillators. *SIAM Journal on Applied Mathematics*, 36(3):509–515, 1979.
- [20] M G Rosenblum, A S Pikovsky, and J Kurths. Phase synchronization of chaotic oscillators. *Physical Review Letters*, 76(11):1804–1807, 1996.
- [21] Réka Albert and Albert-László Barabási. Statistical mechanics of complex networks. *Reviews of Modern Physics*, 74(1):47–97, 2002.
- [22] D J Watts and S H Strogatz. Collective dynamics of ‘small-world’ networks. *Nature*, 393(6684):440–442, 1998.
- [23] Mark D. Humphries and Kevin Gurney. Network ‘Small-World-Ness’: A Quantitative Method for Determining Canonical Network Equivalence. *PLoS ONE*, 3(4):e2051, 2008.
- [24] Qawi K. Telesford, Karen E. Joyce, Satoru Hayasaka, Jonathan H. Burdette, and Paul J. Laurienti. The Ubiquity of Small-World Networks. *Brain Connectivity*, 1(5):367–375, 2011.
- [25] Jeffrey L. Rogers and Luc T. Wille. Phase transitions in nonlinear oscillator chains. *Physical Review E*, 54(3):R2193–R2196, 1996.
- [26] Mikail Rubinov, Rolf J F Ypma, Charles Watson, and Edward T Bullmore. Wiring cost and topological participation of the mouse brain connectome. *Proceedings of the National Academy of Sciences of the United States of America*, 112(32):10032–10037, 2015.
- [27] H. Hong, M. Y. Choi, and Beom Jun Kim. Synchronization on small-world networks. *Physical Review E*, 65(2):1–5, 2002.
- [28] Richard Taylor. There is no non-zero stable fixed point for dense networks in the homogeneous Kuramoto model. *Journal of Physics A: Mathematical and Theoretical*, 45(5):055102, 2012.
- [29] Yuanzhao Zhang and Steven H. Strogatz. Basins with Tentacles. *Physical Review Letters*, 127(19):194101, 2021.

- [30] Alex Townsend, Michael Stillman, and Steven H. Strogatz. Dense networks that do not synchronize and sparse ones that do. *Chaos: An Interdisciplinary Journal of Nonlinear Science*, 30(8):083142, 2020.
- [31] Maximilian Gelbrecht, Jürgen Kurths, and Frank Hellmann. Monte Carlo basin bifurcation analysis. *New Journal of Physics*, 22(3):033032, 2020.
- [32] Franziska Peter and Arkady Pikovsky. Transition to collective oscillations in finite Kuramoto ensembles. *Physical Review E*, 97(3):032310, 2018.
- [33] Dane Taylor, Per Sebastian Skardal, and Jie Sun. Synchronization of Heterogeneous Oscillators Under Network Modifications: Perturbation and Optimization of the Synchrony Alignment Function. *SIAM Journal on Applied Mathematics*, 76(5):1984–2008, 2016.
- [34] Lluís Arola-Fernández, Sergio Faci-Lázaro, Per Sebastian Skardal, Emanuel-Cristian Boghiu, Jesús Gómez-Gardeñes, and Alex Arenas. Emergence of explosive synchronization bombs in networks of oscillators. *Communications Physics*, 5(1):264, 2022.
- [35] R. C. Budzinski, B. R. R. Boaretto, T. L. Prado, R. L. Viana, and S. R. Lopes. Synchronous patterns and intermittency in a network induced by the rewiring of connections and coupling. *Chaos: An Interdisciplinary Journal of Nonlinear Science*, 29(12):123132, 2019.
- [36] Yoshiki Kuramoto. *Chemical Oscillations, Waves, and Turbulence*, volume 19 of *Springer Series in Synergetics*. Springer Berlin Heidelberg, Berlin, Heidelberg, 1984.
- [37] Per Sebastian Skardal and Alex Arenas. Higher order interactions in complex networks of phase oscillators promote abrupt synchronization switching. *Communications Physics*, 3(1):218, 2020.
- [38] Hyunsuk Hong, Jaegon Um, and Hyunggyu Park. Link-disorder fluctuation effects on synchronization in random networks. *Physical Review E - Statistical, Nonlinear, and Soft Matter Physics*, 87(4):1–5, 2013.
- [39] Christopher Rackauckas and Qing Nie. DifferentialEquations.jl – A Performant and Feature-Rich Ecosystem for Solving Differential Equations in Julia. *Journal of Open Research Software*, 5(1):15, 2016.
- [40] Jeff Bezanson, Alan Edelman, Stefan Karpinski, and Viral B Shah. Julia: A fresh approach to numerical computing. *SIAM Review*, 59(1):65–98, 2017.
- [41] John D Hunter. Matplotlib: A 2D Graphics Environment. *Computing in science & engineering*, 9(3):90–95, 2007.
- [42] George Datseris, Jonas Isensee, Sebastian Pech, and Tamás Gál. DrWatson: the perfect sidekick for your scientific inquiries. *Journal of Open Source Software*, 5(54):2673, 2020.
- [43] Karel Rossi. Repository for dynamical malleability code. *Github Repository*, 2022.

- [44] Georgi S. Medvedev. Small-world networks of Kuramoto oscillators. *Physica D: Nonlinear Phenomena*, 266:13–22, 2014.
- [45] Nicole Carlson, Dong-Hee Kim, and Adilson E. Motter. Sample-to-sample fluctuations in real-network ensembles. *Chaos: An Interdisciplinary Journal of Nonlinear Science*, 21(2):025105, 2011.
- [46] Hyunsuk Hong, Hugues Chaté, Hyunggyu Park, and Lei Han Tang. Entrainment transition in populations of random frequency oscillators. *Physical Review Letters*, 99(18):1–4, 2007.
- [47] Hyunsuk Hong, Hyunggyu Park, and Lei-Han Tang. Anomalous Binder Cumulant and Lack of Self-Averageness in Systems with Quenched Disorder. *Journal of the Korean Physical Society*, 49(5):L1885–L1889, 2006.
- [48] Steven H. Strogatz and Renato E. Mirollo. Phase-locking and critical phenomena in lattices of coupled nonlinear oscillators with random intrinsic frequencies. *Physica D: Nonlinear Phenomena*, 31(2):143–168, 1988.
- [49] Jordan G Brankov, Daniel M Danchev, and Nicholai S Tonchev. *Theory of Critical Phenomena in Finite-Size Systems*. World Scientific, 2000.
- [50] Eric J. Hildebrand, Michael A. Buice, and Carson C. Chow. Kinetic Theory of Coupled Oscillators. *Physical Review Letters*, 98(5):054101, 2007.
- [51] Paulo F. C. Tilles, Fernando F. Ferreira, and Hilda A. Cerdeira. Multistable behavior above synchronization in a locally coupled Kuramoto model. *Physical Review E*, 83(6):066206, 2011.
- [52] K. Binder. Finite size effects on phase transitions. *Ferroelectrics*, 73(1):43–67, 1987.
- [53] Per Sebastian Skardal, Dane Taylor, and Jie Sun. Optimal Synchronization of Complex Networks. *Physical Review Letters*, 113(14):144101, 2014.
- [54] Markus Brede. Synchrony-optimized networks of non-identical Kuramoto oscillators. *Physics Letters, Section A: General, Atomic and Solid State Physics*, 372(15):2618–2622, 2008.
- [55] R. Carareto, F. M. Orsatti, and J. R.C. Piqueira. Optimized network structure for full-synchronization. *Communications in Nonlinear Science and Numerical Simulation*, 14(6):2536–2541, 2009.
- [56] Lubos Buzna, Sergi Lozano, and Albert Díaz-Guilera. Synchronization in symmetric bipolar population networks. *Physical Review E*, 80(6):066120, 2009.
- [57] Didier Sornette. *Critical Phenomena in Natural Sciences, Chaos, Fractals, Self-organization and Disorder: Concepts and Tools*. Springer Series in Synergetics. 2006.
- [58] Hyunsuk Hong, Hyunggyu Park, and Lei Han Tang. Finite-size scaling of synchronized oscillation on complex networks. *Physical Review E*, 76(6):1–7, 2007.

- [59] Shai Wiseman and Eytan Domany. Lack of self-averaging in critical disordered systems. *Physical Review E*, 52(4):3469–3484, 1995.
- [60] M E Newman and D J Watts. Scaling and percolation in the small-world network model. *Physical Review E*, 60(6 Pt B):7332–7342, 1999.
- [61] Victor Buenda, Pablo Villegas, Raffaella Burioni, and Miguel A. Muoz. The broad edge of synchronization: Griffiths effects and collective phenomena in brain networks. *Philosophical Transactions of the Royal Society A*, 380(2227):20200424, 2022.
- [62] Pablo Villegas, Paolo Moretti, and Miguel A. Muñoz. Frustrated hierarchical synchronization and emergent complexity in the human connectome network. *Scientific Reports*, 4(1):5990, 2014.
- [63] G Tononi, O Sporns, and G M Edelman. A measure for brain complexity: relating functional segregation and integration in the nervous system. *Proceedings of the National Academy of Sciences*, 91(11):5033–5037, 1994.
- [64] Giulio Tononi and Gerald M. Edelman. Consciousness and Complexity. *Science*, 282(5395):1846–1851, 1998.
- [65] Gustavo Deco, Giulio Tononi, Melanie Boly, and Morten L. Kringelbach. Rethinking segregation and integration: contributions of whole-brain modelling. *Nature Reviews Neuroscience*, 16(7):430–439, 2015.
- [66] Andrew A Fingelkurts and Alexander A Fingelkurts. Timing in cognition and EEG brain dynamics: discreteness versus continuity. *Cognitive Processing*, 7(3):135–162, 2006.
- [67] Cheng-yu T. Li, Mu-ming Poo, and Yang Dan. Burst Spiking of a Single Cortical Neuron Modifies Global Brain State. *Science*, 324(5927):643–646, 2009.
- [68] Lyle Muller, Ján Mináč, and Tung T. Nguyen. Algebraic approach to the Kuramoto model. *Physical Review E*, 104(2):L022201, 2021.
- [69] Roberto C. Budzinski, Tung T. Nguyen, Jacqueline Doàn, Ján Mináč, Terrence J. Sejnowski, and Lyle E. Muller. Geometry unites synchrony, chimeras, and waves in nonlinear oscillator networks. *Chaos*, 32(3):031104, 2022.
- [70] Edward J. Hancock and Georg A. Gottwald. Model reduction for Kuramoto models with complex topologies. *Physical Review E*, 98(1):012307, 2018.
- [71] Steven Strogatz. *Sync: The Emerging Science of Spontaneous Order*. Hyperion Press, 2003.
- [72] Ulrike Feudel. Complex Dynamics In Multistable Systems. *International Journal of Bifurcation and Chaos*, 18(06):1607–1626, 2008.
- [73] Alexander N. Pisarchik and Alexander E. Hramov. Multistability in Physical and Living Systems, Characterization and Applications. *Springer Series in Synergetics*, 2022.

- [74] Peter J. Menck, Jobst Heitzig, Norbert Marwan, and Jürgen Kurths. How basin stability complements the linear-stability paradigm. *Nature Physics*, 9(2):89–92, 2013.
- [75] Hana Krakovská, Christian Kuehn, and Iacopo P Longo. Resilience of dynamical systems. *European Journal of Applied Mathematics*, pages 1–46, 2023.
- [76] Silvan Hürkey, Nelson Niemeyer, Jan-Hendrik Schleimer, Stefanie Ryglewski, Susanne Schreiber, and Carsten Duch. Gap junctions desynchronize a neural circuit to stabilize insect flight. *Nature*, 618(7963):118–125, 2023.
- [77] K. L. Rossi, R. C. Budzinski, B. R. R. Boaretto, T. L. Prado, U. Feudel, and S. R. Lopes. Phase-locking intermittency induced by dynamical heterogeneity in networks of thermosensitive neurons. *Chaos: An Interdisciplinary Journal of Nonlinear Science*, 31(8):083121, 2021.
- [78] Everton S. Medeiros, Rene O. Medrano-T, Iberê L. Caldas, and Ulrike Feudel. Boundaries of synchronization in oscillator networks. *Physical Review E*, 98(3):030201, 2018.
- [79] George Datseris. DynamicalSystems.jl: A Julia software library for chaos and nonlinear dynamics. *Journal of Open Source Software*, 3(23):598, 2018. Publisher: The Open Journal.
- [80] Merten Stender and Norbert Hoffmann. bSTAB: an open-source software for computing the basin stability of multi-stable dynamical systems. *Nonlinear Dynamics*, pages 1–18, 2021.
- [81] George Datseris, Kalel Luiz Rossi, and Alexandre Wagemakers. Framework for global stability analysis of dynamical systems. *Chaos: An Interdisciplinary Journal of Nonlinear Science*, 33(7):073151, 2023.
- [82] Ying-Cheng Lai and Tamás Tél. *Transient Chaos: Complex Dynamics on Finite-Time Scales*. Applied Mathematical Sciences. Springer New York, NY, 2009.
- [83] Alan Hastings, Karen C. Abbott, Kim Cuddington, Tessa Francis, Gabriel Gellner, Ying-Cheng Lai, Andrew Morozov, Sergei Petrovskii, Katherine Scranton, and Mary Lou Zeeman. Transient phenomena in ecology. *Science*, 361(6406), 2018.
- [84] A. M. Turing. On Computable Numbers, with an Application to the Entscheidungsproblem. *Proceedings of the London Mathematical Society*, s2-42(1):230–265, 1937.
- [85] George S. Boolos, John P. Burgess, and Richard C. Jeffrey. *Computability and Logic*. Cambridge University Press, 5 edition, 2007.
- [86] Claire M. Postlethwaite, Peter Ashwin, and Matthew Egbert. A Continuous Time Dynamical Turing Machine. *IEEE Transactions on Neural Networks and Learning Systems*, PP(99):1–13, 2024.
- [87] Peter Ashwin and Marc Timme. When instability makes sense. *Nature*, 436(7047):36–37, 2005.

- [88] Ofer Mazor and Gilles Laurent. Transient Dynamics versus Fixed Points in Odor Representations by Locust Antennal Lobe Projection Neurons. *Neuron*, 48(4):661–673, 2005.
- [89] Emmanuelle Tognoli and J. A.Scott Kelso. The Metastable Brain. *Neuron*, 81(1):35–48, 2014.
- [90] B. A. W. Brinkman, H. Yan, A. Maffei, I. M. Park, A. Fontanini, J. Wang, and G. La Camera. Metastable dynamics of neural circuits and networks. *Applied Physics Reviews*, 9(1):011313, 2022.
- [91] Daniel Koch, Akhilesh Nandan, Gayathri Ramesan, and Aneta Koseska. Biological computations: Limitations of attractor-based formalisms and the need for transients. *Biochemical and Biophysical Research Communications*, 720:150069, 2024.
- [92] Saurabh Vyas, Matthew D. Golub, David Sussillo, and Krishna V. Shenoy. Computation Through Neural Population Dynamics. *Annual Review of Neuroscience*, 43(1):249–275, 2020.
- [93] David Sussillo and Omri Barak. Opening the Black Box: Low-Dimensional Dynamics in High-Dimensional Recurrent Neural Networks. *Neural Computation*, 25(3):626–649, 2013.
- [94] D. Koch, A. Nandan, G. Ramesan, I. Tyukin, A. Gorban, and A. Koseska. Ghost Channels and Ghost Cycles Guiding Long Transients in Dynamical Systems. *Physical Review Letters*, 133(4):047202, 2024.
- [95] Akhilesh Nandan, Abhishek Das, Robert Lott, and Aneta Koseska. Cells use molecular working memory to navigate in changing chemoattractant fields. *eLife*, 11:e76825, 2022.
- [96] Laura N. Driscoll, Krishna Shenoy, and David Sussillo. Flexible multitask computation in recurrent networks utilizes shared dynamical motifs. *Nature Neuroscience*, 27(7):1349–1363, 2024.
- [97] Rodrigo Laje and Dean V Buonomano. Robust timing and motor patterns by taming chaos in recurrent neural networks. *Nature Neuroscience*, 16(7):925–933, 2013.
- [98] Lauren M. Jones, Alfredo Fontanini, Brian F. Sadacca, Paul Miller, and Donald B. Katz. Natural stimuli evoke dynamic sequences of states in sensory cortical ensembles. *Proceedings of the National Academy of Sciences*, 104(47):18772–18777, 2007.
- [99] Giancarlo La Camera, Alfredo Fontanini, and Luca Mazzucato. Cortical computations via metastable activity. *Current Opinion in Neurobiology*, 58:37–45, 2019.
- [100] Peter Ashwin and Claire Postlethwaite. Excitable networks for finite state computation with continuous time recurrent neural networks. *Biological Cybernetics*, 115(5):519–538, 2021.

- [101] Peter Ashwin, Muhammed Fadera, and Claire Postlethwaite. Network attractors and nonlinear dynamics of neural computation. *Current Opinion in Neurobiology*, 84:102818, 2024.

Acknowledgments

Doing a PhD is not trivial (no citation needed here, I think). It is made possible not just from one's own hard work, but with help and support from many others.

To start, the PhD was possible due to financial support from the German Academic Exchange Foundation (DAAD, in german). I am very thankful for the opportunity to do all this work with their warm support. In this sense, I am also grateful to the University of Oldenburg for the structures provided that allowed me to work.

Moving from the material to the intellectual and personal support, I am extremely grateful to Prof. Ulrike Feudel, my supervisor for all of these years! We had a lot of fun, and I learned so much from her. On top of the specific knowledge of the area, I think maybe the most important skill she developed on me was the ability to refine a thought and rigorously develop an idea until you are confident about it. On top of all the actual science we made, I find it amazing how many conferences I had the opportunity to participate in, and how many people I met - a lot of this I owe to Ulrike's support. In a similar vein I also want to deeply thank my friend and collaborator, Prof. (yes, Prof!) Everton Medeiros. Maybe without even noticing, he also taught me so much. He was a crucial aid in making this whole process a lot more fun and exciting - with, of course, better science. I will always remember this fondly - as will I remember his legendary goal from the corner of the pitch in Spiekeroog. Football's loss is academia's gain. Finally, since my Bachelor's I've always been able to count on my friends and collaborators Roberto Budzinski and Bruno Boaretto. I've counted on them for endless scientific discussions, arguments about how something should be written on a paper, and motivation. All of this always with a really nice and fun atmosphere.

Moving more to the emotional (and personal still) support, I am above all thankful to my mom and my sister for just about everything. Moving abroad is not easy - for anyone involved - but their unwavering love, warmth, and understanding made it all happen! This extends to my whole family, in fact.

Friends are also a crucial ingredient to a nice life. And in this I also have had the luck to count on some amazing figures. I will only name some - their egos will have to be satisfied. In no particular order I want to thank from the bottom of my heart Jakob and Bianca Weik, Maira Theisen, Gabriel Gubert, Lucas Polyceno, Carlos Martins, Alexandre Camargo, Rafa Jakuboski, Joao Paludo, Marcos Sato, George Datseris, Bryony Hobden, Patryk Bielski, Luis Gustavo, and Deoclecio Valente - and many others I equally love but, come on, the list was already too big.

Finally, I mentioned I met a lot of amazing people doing science, some of whom I already mentioned. For all the discussions, support, and fun, I want to especially thank Klaus Lehnertz, Lyle Muller, Pete Ashwin, Aneta Koseska, Vyacheslav Kruglov, Ryan Deeley, and Jan Freund.

Eidesstattliche Erklärung

Hiermit versichere ich, dass ich diese Dissertation selbstständig verfasst habe und nur die hier angegebenen Hilfsmittel und Quellen benutzt habe. Zudem versichere ich, dass diese Dissertation weder in ihrer Gesamtheit noch in Teilen einer anderen Hochschule zur Begutachtung in einem Promotionsverfahren vorliegt oder vorgelegen hat. Bis auf die angegebenen Teilpublikationen, ist diese Arbeit noch nicht veröffentlicht worden. Die Leitlinien guter wissenschaftlicher Praxis an der Carl von Ossietzky Universität Oldenburg wurden befolgt. Für dieses Promotionsvorhaben wurden keine kommerziellen Vermittlungs- oder Beratungsdienste in Anspruch genommen.

Oldenburg, den 07.11.2024

Kalel Luiz Rossi